NORTHWESTERN UNIVERSITY

Determining the Brainstem's Role in Loss of Independent Joint Control in Chronic Stroke

A DISSERTATION

SUBMITTED TO THE GRADUATE SCHOOL IN PARTIAL FULFILLMENT OF THE
REQUIREMENTS

For the degree

DOCTOR OF PHILOSOPHY

Field of Neuroscience

By

Meriel Ann Owen

EVANSTON, ILLINOIS

December 2017

Abstract

Following a stroke, precise, individuated control of single joints is often replaced by highly stereotyped patterns of multi-joint movement, due to a loss of independent joint control, which can negatively impact functional use of the paretic arm. Despite the debilitating nature of this impairment, the precise underlying neural mechanisms remain uncertain. Previous research has suggested that following stroke-induced damage to descending motor pathways in the lesioned hemisphere, contralesional corticobulbospinal pathways, such as the corticoreticulospinal pathway, become more heavily relied upon; however, these pathways have not been studied directly in human stroke individuals. Therefore, the goal of this work is first to determine whether structural and functional neuroanatomical correlates of the corticoreticulospinal tract are altered in chronic hemiparetic stroke when compared to healthy, age-matched controls and second, to determine whether structural and functional neural changes are directly related to loss of independent joint control in chronic stroke.

This work combines multi-modal neuroimaging with rehabilitation robotics to determine whether brain structure and function in chronic stroke support the hypothesis of increased reliance on contralesional cortico-reticulospinal pathways contributing to loss of independent joint control. Three types of MR imaging are used to assess structure (white matter and gray matter) and function in both chronic stroke and healthy control individuals.

In the lesioned hemisphere, stroke individuals display evidence of white matter damage and degeneration when compared with controls. However, in the contralesional hemisphere, stroke individuals display evidence of increased white matter microstructural integrity. This effect is particularly evident in those individuals with the greatest levels of motor impairment.

Resting state functional connectivity is increased in stroke when compared to controls, and gray matter integrity in the contralesional motor cortex is also increased in the most severely impaired individuals. Finally, specific contralesional neural substrates correlate significantly with a quantitative robotic measurement of loss of independent joint control.

This work demonstrates direct evidence for increased reliance on contralesional corticoreticulospinal pathways in chronic hemiparetic stroke, especially in the most severely impaired individuals. It emphasizes a need to better understand the neuroplastic changes that occur over time in the brain after stroke, particularly in the brainstem, in order to eventually be able to design more patient-specific and targeted therapeutic interventions.

Acknowledgements

This work would not have been possible without all the incredible people who have helped and supported me along the way. I would like to thank my mentor, Jules Dewald for all of his guidance and support throughout my graduate career. I came in with a specific vision for a neuroimaging project, and I have been lucky to have had his support and guidance through study design, obtaining funding, data collection and publication. I'm grateful to have been given the freedom to pursue a project I was excited about. Jules has a deep passion for combining quantitative engineering approaches with neuroscience to find new ways to help patients. It has been a real privilege to have been a part of this, and I have learned so much from him.

Thank you to my committee members who have helped shape and strengthen my project along the way. I have really enjoyed seeing the project evolve from your thoughtful questions and insightful comments. Through my first rotation, every committee meeting and professional guidance, Todd Parrish has always provided helpful advice and deep technical expertise in neuroimaging. Xue Wang always provided neuroimaging assistance by answering my processing questions. Mike Ellis taught me how to use robotics to approach a scientific question and provided invaluable clinical expertise. Lee Miller was always available for a chat about brainstem anatomy and a healthy dose of neuroimaging skepticism. Carson Ingo has been an immense help in the technical weeds of neuroimaging. He has helped me to think more critically about my research, improve my writing and help me publish my work. A big thanks to Jim Elliott for reaching out and helping me get authored on my first paper. Your collaborative and friendly personality have been hugely influential and helpful.

Thank you to my friends for always supporting me even when things got difficult. Xiaowen Yu, Eileen McIver, Agnes Bao, Seoan Huh, Osefame Ewaleifoh, Christina Young, Amanda Herrera, Alissa Mrazek, my NU friends, thank you so much for always being there to share stories, offer support and adventure in Chicago. To my girls at home, thank you for the decades of friendship. I can't express how much strength you have all given me throughout this process.

Thank you to my parents and grandparents for always supporting me. You have consistently helped me keep perspective, shared in the successes and failures, and stood by me, no matter what. To my sister, Mallory, thank you for always listening to me, for hours of talks about our science dreams, for your editing services and most of all, for your friendship. I'm so excited to continue to share neuroscience with you as you progress through medical school.

Lastly, I thank Mark Addison. I feel deep gratitude for your support through every step of this process: the applications, the interviews, a move to Chicago, 6 years of hard work and years of long distance. It has been a crazy adventure, but your unwavering support has been a steady rock that has kept me going. Thank you for always believing in me, even when I didn't.

Dedication

I dedicate this work to Thomas Huw Owen and Jonathan Harms.

Someday we will better understand the complexities of the human brain.

You are deeply missed.

Table of Contents

List of Figures

List of Tables

1. Introduction

"We have a brain for one reason and one reason only -- that's to produce adaptable and complex movements. Movement is the only way you have of affecting the world around you. Communication—speech, gestures, writing, sign language—they're all mediated through contractions of your muscles. Sensory, memory and cognitive processes are all important, but they're only important to either drive or suppress future movements. There can be no evolutionary advantage to laying down memories of childhood or perceiving the color of a rose if it doesn't affect the way you're going to move later in life."

--Daniel Wolpert

The human brain is made up of over 100 billion neurons. It is perhaps the most complex structure in the body, and production of movement is arguably its most important purpose. The system that controls movement, the motor system, is a set of neural structures that generate the commands that act on muscles, causing them to contract and generate movement. Because most of the activities humans carry out on a daily basis, in some way or another, depend on specific and effective motor control, neural injury, such as stroke, can be devastating.

There are as many as 1.1 million hemiparetic stroke survivors in the U.S. who exhibit movement impairments. One fundamental example of movement impairment is the loss of independent joint control, which results in a stereotypic multi-joint movement pattern consisting of abnormal coupling between shoulder abduction and elbow, wrist, and finger flexion. Research using an ACT^{3D} robotic device, used to increase shoulder abduction loading, has demonstrated that this loss of independent joint control has a negative impact on reaching ability (Ellis *et al.*, 2011) and hand opening (Lan, 2017), both critical components of functional use of the arm during daily activities. Despite the debilitating nature of this motor impairment and its negative

effect on recovery of upper limb function following stroke, we still have incomplete evidence of the underlying neural mechanisms of its development.

The human motor system contains multiple descending pathways that link the brain to the spinal cord, allowing transmission of commands for voluntary movement. Because the motor system consists of multiple distributed and parallel systems, lesions can degrade but not completely eliminate its function. After a stroke, brain edema and subsequent inflammation occur, initiating a complex cascade of cellular and molecular processes, not only in the area surrounding the lesion but also in remote brain regions. These processes lead to cerebral reorganization or "rewiring" in surviving networks that can cause some spontaneous recovery of function. Despite the brain's ability for some motor relearning and neuroplasticity, the chronic stroke brain depends on remaining motor pathways that may not be as effective at communicating motor signals to the spinal cord as the intact brain.

Much of the currently available information about neuroanatomical connections comes from studies in animals. Since techniques such as axonal transport or immunohistochemistry cannot be used in humans, a gap in knowledge exists especially with regard to smaller tracts and fibers. Despite this limitation, work done in nonhuman primates can serve as a good foundation for what is likely to happen in the human brain after stroke.

Of particular interest is the role of the contralesional hemisphere (ipsilateral to the paretic limb) and its influence on descending pathways in contributing to motor control after stroke. In healthy primates, direct ipsilateral corticospinal pathways appear absent for hand muscles. For this reason, ipsilateral corticospinal pathways from the contralesional hemisphere are considered of little importance for recovery of function. In contrast, inputs from pathways originating in the

brainstem nuclei become strongly enhanced (2.5x) in forearm flexors after a stroke. This finding supports earlier work done in human stroke individuals that demonstrates a contralesional oligosynaptic corticobulbospinal connection using brain stimulation techniques (Schwerin *et al.*, 2008; Schwerin *et al.*, 2011). Evidence in both animals and humans suggests that in the absence of pyramidal tracts, the brainstem pathways are capable of controlling a wide range of activity. Bulbospinal pathways may be able to convey ipsilateral motor signals after injury. The pattern of reorganization in humans, with respect to these bulbospinal pathways, still remains to be studied in detail.

However, there is increasing evidence from advances in neuroimaging that similar neuroplastic changes occur in humans as in nonhuman primates in response to neural injury. Neuroimaging allows us to probe the human brain in vivo to provide a greater understanding of the mechanisms of recovery. Functional magnetic resonance imaging (fMRI) studies confirm that movements of the paretic limb are associated with enhanced neural activity in both the lesioned and non-lesioned (contralesional) hemispheres; however, previous studies of motor tasks remain limited because they often look at joints in isolation rather than in the context of the whole limb.

Much of the neuroimaging work done in humans focuses on the motor cortex and the descending corticospinal tract, but as animal studies demonstrate, many critical aspects of movement control are performed by structures and pathways positioned below the cerebral hemispheres. The pathways that project from the brainstem to the spinal cord provide additional avenues for both hemispheres to influence movements of the paretic limb, which has important implications for recovery of function following injury. These bulbospinal pathways remain

understudied in humans, and it remains speculative whether they play a role in abnormal joint coupling after stroke.

Cerebral reorganization undoubtedly contributes to functional recovery after stroke, but it is unclear what role the brainstem structures and pathways play in humans. Therefore, the purpose of this work is to determine whether structural and functional changes occur within the brainstem in chronic hemiparetic stroke individuals when compared to healthy, age-matched control individuals and if so, to relate these changes to a quantitative robotic measurement of abnormal joint coupling in the paretic limb. To date, many studies have tested the efficacy of rTMS or tDCS for enhancing recovery post-stroke. Results using these approaches have shown temporary changes in motor performance but have not resulted in significant and sustained improved outcomes following stroke. It may be that a better understanding of the role the brainstem plays in neural reorganization and motor control post-stroke could help design and rationalize future therapeutic strategies aimed at diminishing or even preventing the debilitating effects of loss of independent joint control in human stroke patients.

2. Background and Literature Review

The following review will provide an overview of stroke and the main impairment that follows: loss of independent joint control. It will outline the major anatomical and physiological principles of the human motor system in health and disease followed by a description of several imaging methods used to examine it.

Stroke

A stroke occurs in the brain when a blood vessel is blocked, prohibiting blood flow to neural tissue (ischemic stroke) or when there is bleeding in the brain (hemorrhagic stroke). In the time immediately following a stroke, brain edema can occur, typically reaching its peak in the following 3-5 days (Shaw *et al.*, 1959). This brain edema can temporarily leave neural pathways unable to effectively transmit signals and more permanently leads to a toxic molecular cascade, neuronal cell death, and subsequent poor functional outcomes (Battey *et al.*, 2014). Of all strokes, 87% are ischemic and 13% hemorrhagic (GCNKSS, NINDS, 1999). It is estimated that in 2010, the global prevalence of stroke was 33 million, with 16.9 million people having a first time stroke (Mozaffarian *et al.*, 2016).

On average, someone in the United States has a stroke every forty seconds, and someone dies of a stroke every four minutes, costing an estimated $36.5 billion each year (Go *et al.*, 2014). It is the leading cause of long term disability, leaving survivors with motor, language, cognitive and other impairments. Most patients do show some degree of recovery; however, there is no universally accepted treatment (Ward & Cohen, 2004) and few people return to pre-stroke state (Cramer & Chopp, 2000). Although rehabilitation techniques aimed at adaptation to

impairment are well recognized, strategies designed to restore function are less well developed. It is necessary to have better understanding of the factors that promote central nervous system reorganization post-stroke and the role this reorganization plays in recovery of function. This information would help facilitate the development of novel, evidence-based therapeutic techniques that could better optimize recovery.

Healthy Motor System

Stroke often causes damage to the motor system, which comprises a complicated network of connections within itself and other parts of the nervous system. It can become altered both directly from stroke-induced damage and in compensatory reorganization in response to such a focal injury. Understanding how a damaged brain adapts following neural injury, such as a stroke, can shed light on the structural and functional organization of the healthy human motor system.

Cortical Regions

There are several motor areas included in the cortical motor system, each one with its own set of corticospinal neurons (Dum & Strick, 1991). These include primary motor cortex (M1), premotor cortex (PM), supplementary motor area (SMA) and cingulate motor cortex, shown in Figure 2.1. M1 lies along the pre-central gyrus, in Brodmann's area 4, and is important for the neural impulses that produce movement through projections of the corticospinal tract (CST) (Dum & Strick, 1991). Historically, it was believed that M1 was the primary origin of cortical commands to the spinal cord, with premotor areas primarily responsible for integrating information from parietal and frontal regions and sending that information to M1; however, careful anatomical retrograde tracing in primates has shown that premotor areas (PM, SMA,

cingulate) have the potential to influence the control of movement not only at the level of M1 but also directly through projections to the spinal cord, which, when combined, equal or even outnumber those from M1 (Dum & Strick, 2002).

Secondary motor areas have some degree of somatotopic representation (Dum & Strick, 2002) and are thought to be active in higher order aspects of motor control. More specifically in primates, PM cortex has been associated with motor preparation of externally guided reaching (Cisek & Kalaska, 2005; Churchland *et al.*, 2006) and shaping the hand around an object during grasp (Murata *et al.*, 1997). In contrast, SMA activity has been associated with preparation of
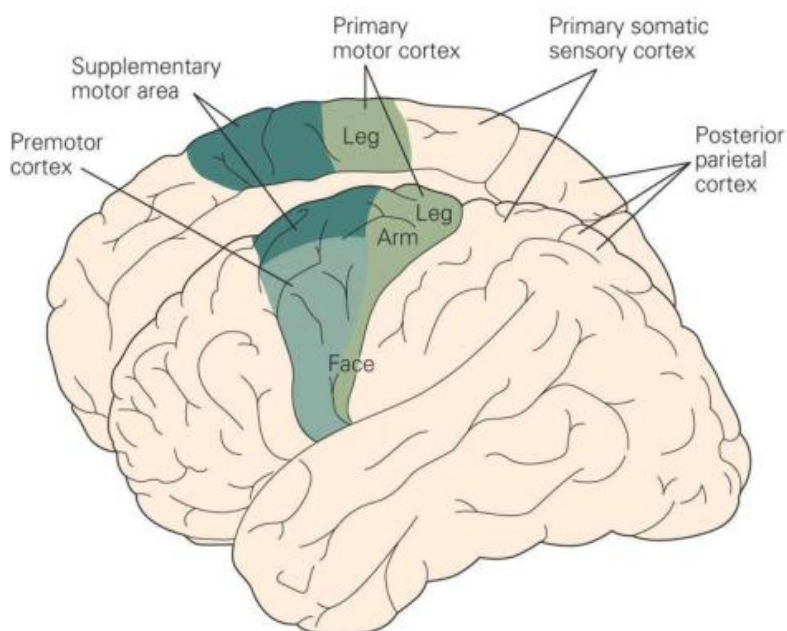
Figure 2.1
Based on their histological studies at the beginning of the 20th century, Korbinian Brodmann and Alfred Campbell each divided the precentral cortex in humans into two anatomically distinct cytoarchitectonic areas: the primary motor cortex (Brodmann's area 4) and premotor cortex (Brodmann's area 6). Subsequent studies by Woolsey and colleagues led to subdivision of the premotor cortex into medial and lateral halves, the supplementary area and lateral premotor cortex, respectively (Kandel, 2013).

self-initiated movements (Erdler *et al.*, 2000) and plays an important role in motor imagery (Kuhtz-Buschbeck *et al.*, 2003). Together, these cortical regions coordinate to send commands that ultimately control activity of motor neurons in the spinal cord.

Other cortical inputs targeting the motor cortex originate from the opposite hemisphere and project through the corpus callosum. Cortical motor regions also receive projections from the basal ganglia (Hoover & Strick, 1993) and cerebellum (Middleton & Strick, 1998) by way of the thalamus, forming reciprocal connections and a complicated cortical-subcortical network that generates movement. Descending cortical and subcortical pathways to the spinal cord constitute the primary routes by which the brain can control spinal motor output. Descending corticobulbar pathways influence motor control through projections to brainstem structures, which give rise to bulbospinal pathways discussed below.

Corticospinal tract (CST)

The cortical projections terminating in the spinal cord comprise the corticospinal tract, a large bundle of fibers containing close to a million axons, which spans the length of the brain. In primates, this pathway originates from M1, dorsal and ventral PM cortices, SMA and cingulate motor areas (Dum & Strick, 2005), as well as posterior parietal cortex and parietal operculum (Lemon, 2008). A recent diffusion imaging study in humans demonstrates the contributions of various cortical areas to the corticospinal tract: M1, S1, SMA and PM cortices account for 37%, 32%, 25% and 7% of axons, respectively (Seo & Jang, 2013). From the cortex, the corticospinal tract travels through the internal capsule and cerebral peduncles of the midbrain and decussates in the pyramids of the medulla, resulting in contralateral motor control: the left side of the brain controlling the right side of the spinal cord, and vice versa (Welniarz *et al.*, 2017). A small

percentage of axons do not cross at the pyramids and project ipsilaterally as the anterior corticospinal tract. Corticospinal projections terminate in the spinal cord to make powerful, monosynaptic connections directly with alpha motor neurons in the ventral horn or interneurons that influence those alpha motor neurons. There is evidence that the direct, monosynaptic projections from the cortex to alpha motor neurons in the spinal cord, or cortico-motoneuronal
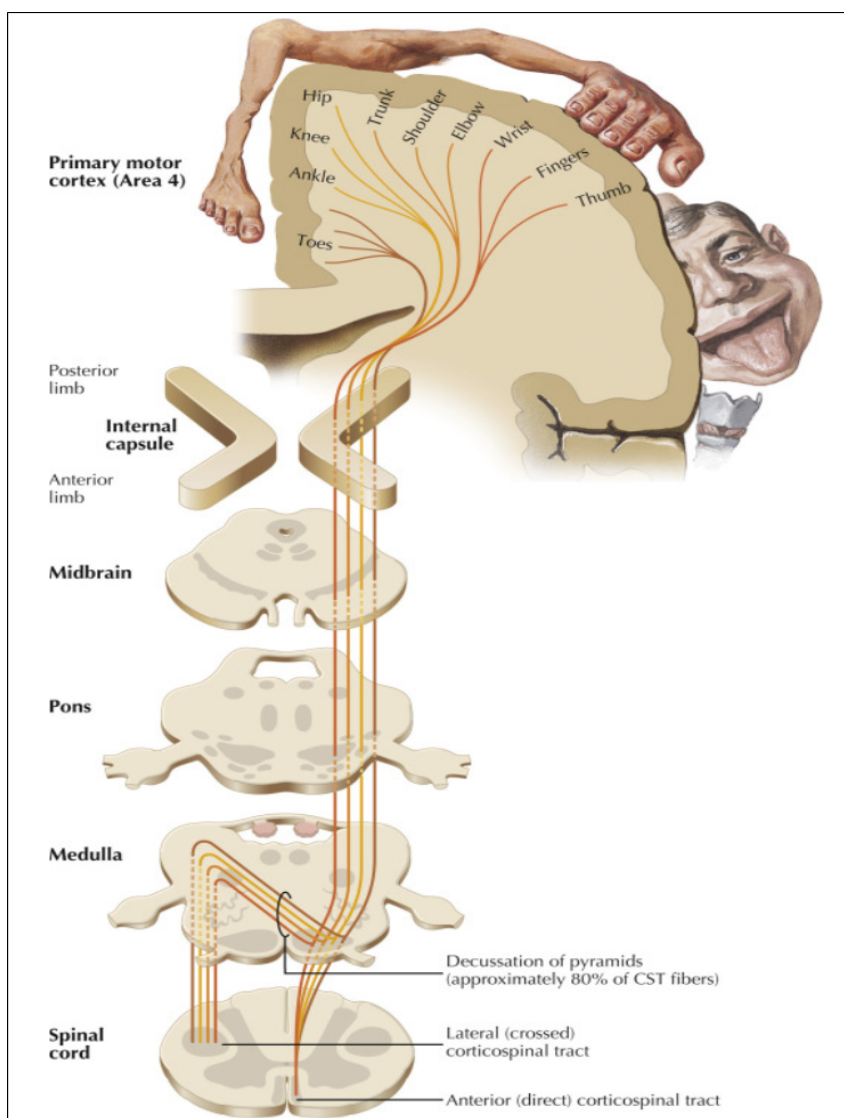
Figure 2.2
Descending trajectory of the corticospinal tract (Felten & Józefowicz, 2003)

connections, observed in non-human primates also exist in humans, with the most pronounced

effects present in the distal muscles (Lemon, 2008). Seminal work by Lawrence and Kuypers

shows that a lesion to the corticospinal tract causes a loss of individuated wrist and finger

movements, demonstrating the pathway's importance in control of distal extremities and fine

finger coordination (Lawrence & Kuypers, 1968a). The neuroanatomical trajectory of the

corticospinal tract is shown in Figure 2.2.

Reticulospinal tract (RetST)

Much of what is known regarding reticulospinal pathway anatomy and function comes

from animal studies, leaving it relatively unstudied in humans. These pathways originate in the

brainstem reticular formation nuclei in the pons and medulla: pontis caudalis, pontis oralis,

parvocellularis, magnocellularis and gigantocellularis (Butler, 2005). Descending axons from

these nuclei travel primarily in the medial longitudinal fasciculus and terminate in the spinal

cord, where they can influence alpha and gamma motor neurons, contributing to skeletal muscle

tone and somatic reflexes (Conn, 2008). The reticulospinal tract tends to facilitate flexors and

suppress extensors ipsilaterally (Davidson & Buford, 2006; Davidson *et al.*, 2007)

Initial work characterizing the reticulospinal tract focused on its role in gross movements

such as locomotion (Mori *et al.*, 2001) and postural stability (Schepens *et al.*, 2008); however,

more recent work in primates shows that it makes mono- and di-synaptic connections to motor

neurons in the forearm (Riddle *et al.*, 2009). Interneurons involved in controlling the hand often

receive convergent information from both the corticospinal tract and the reticulospinal tract

(Riddle & Baker, 2010), and stimulating the reticulospinal tract elicits excitatory post-synaptic

potentials (EPSPs) in hand muscles, albeit much smaller in magnitude than EPSPs resulting from stimulation of the CST (Baker, 2011).

Anatomical tracing studies show cortical regions send bilateral projections to the ponto-medullary reticular formation (PMRF) in both cats and monkeys (Keizer & Kuypers, 1984, 1989). A recent study describes the specific patterns of the corticoreticular projection in macaque monkeys. Anterograde tracer, BDA, was injected into M1, PM or SMA cortical regions, and the labeling of axons was subsequently analyzed on brainstem histological sections. The projections from PM and SMA regions tended to end mainly ipsilaterally in PMRF but contralaterally when originating in M1, and the projections were more dense coming from secondary areas (PM, SMA) compared to M1. The main termination locations corresponded to regions where reticulospinal cell bodies were located, suggesting the existence of a polysynaptic cortico-reticulo-spinal projection in non-human primates (Fregosi *et al.*, 2017b). The corticoreticular pathway can also be detected in humans using diffusion tractography (Jang & Seo, 2014). The more bilateral nature of the reticulospinal system, as opposed to the primarily contralateral distribution of the corticospinal tract, makes it a promising alternative pathway for ipsilateral cortical control of arm movement after neural injury. This anatomical evidence suggests the corticoreticulospinal pathway allows the brain access to motor neurons of the paretic limb from the non-damaged hemisphere, but its output may be constrained to limited motor control.

Rubrospinal tract (RubST)

Evidence from animal models shows that the rubrospinal tract originates in the magnocellular red nucleus in the midbrain. The pathway decussates and descends down to terminate in the rostral part of the spinal cord (Conn, 2008), and it is considered important for

providing additional drive for movements in the elbow and wrist (Lemon, 2008). Despite this

evidence in animal models, it has been argued that in humans, the rubrospinal tract is small and

may not reach the cervical enlargement of the spinal cord (Nathan & Smith, 1982).

Lesion studies in primates demonstrate the relative contributions of these three

descending motor pathways: corticospinal, reticulospinal and rubrospinal. These pathways are

shown in Figure 2.3. A lesion to the corticospinal tract, not involving the cortical projections to
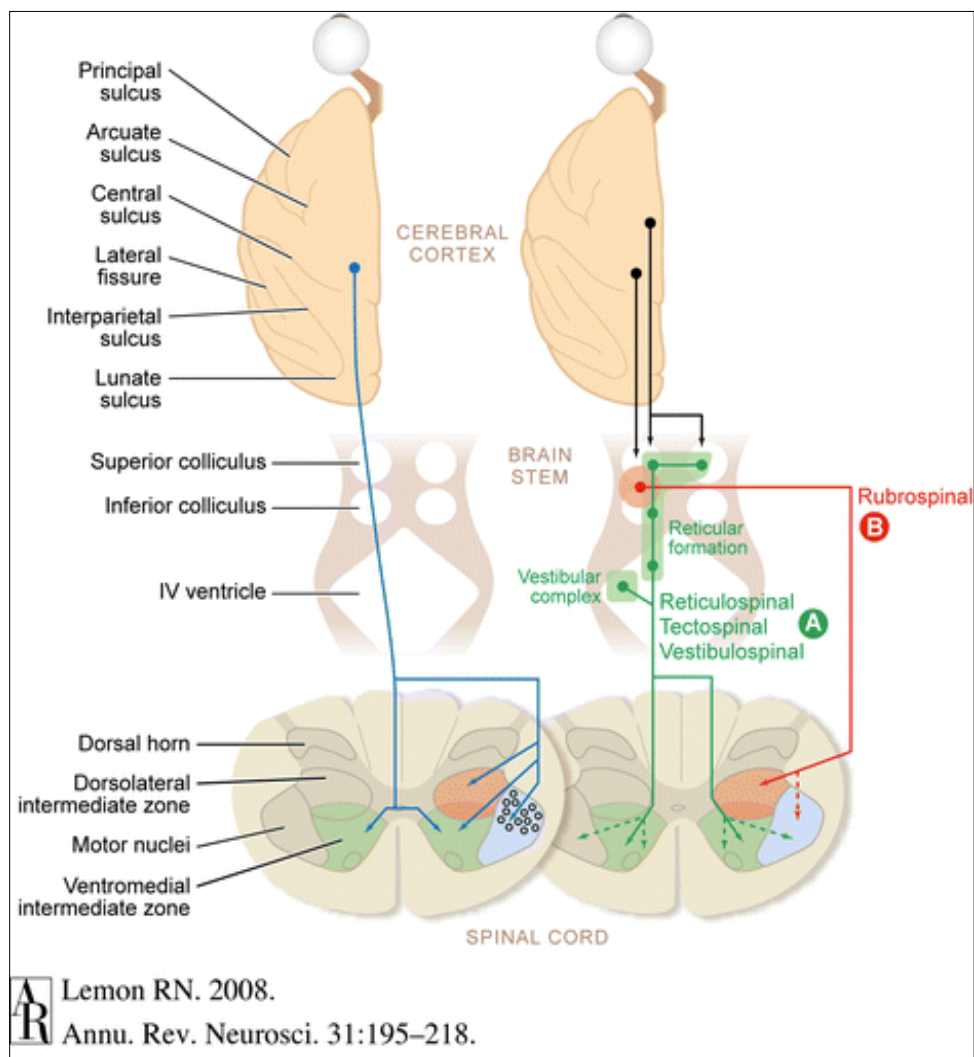
Figure 2.3
Descending pathways of the motor system.

the lower brainstem, causes impairment in independent finger movement; however, gross voluntary motor control remains preserved (Lawrence & Kuypers, 1968a). An additional lesion to the rubrospinal tract causes an inability to initiate independent hand and wrist movements; however, the animals could still climb the bars of their cage, walk, feed and maintain balance (Lawrence & Kuypers, 1968b), emphasizing the importance of remaining intact reticulospinal tract contributions to motor control.

All of these motor areas and pathways make up a complex network that together produce movement. If any single node is damaged or compromised, it is unlikely that one region will be able to replace it; however, other regions may be able to take on new roles in order to help compensate for the loss. The exact nature of compensatory changes in the human brain after neural injury remains unknown, and stroke-induced changes in bulbospinal pathways, such as the reticulospinal and rubrospinal tracts, have not been well described in humans.

Dysfunction in the Motor System after Stroke

Functional Consequences

When corticofugal pathways are damaged following a stroke, functional consequences follow. Hemiparetic stroke is often accompanied by abnormalities in muscle tone, hyperactive stretch reflexes or spasticity, muscle weakness and losses of independent joint control or abnormal movement synergies. Spasticity and weakness are easily detected and have been intensely studied; however, losses in independent joint control that emerge post-stroke often result in greater impairment levels and are the least understood (Dewald *et al.*, 2001). Atypical muscle synergies give rise to stereotypic and abnormal movement patterns that are functionally debilitating (Given *et al.*, 1995). Studies investigating reaching ability post-stroke have shown a

severe loss of independent joint control when individuals support the paretic arm against gravity (Beer *et al.*, 2004), a loss that cannot be accounted for by simple weakness and/or presence of spasticity. This loss of independent joint control, resulting from abnormal coupling between shoulder abduction and elbow, wrist and finger flexion, significantly reduces workspace area (Sukal *et al.*, 2007) and hand opening (Lan, 2017) and serves as a significant source of impairment post-stroke. Understanding the mechanisms behind this debilitating emergence of abnormal joint coupling would help lay the foundation for better maximizing functional recovery in the upper extremity post-stroke.

Neural Consequences

Advances in neuroimaging techniques and knowledge of neuroanatomy have made it clear that cortical and subcortical lesions disrupt descending motor pathways, such as the corticobulbar pathways and the corticospinal tract, shown in blue in Figure 2.3 (Lemon, 2008). Since corticospinal pathways are known to be important for control of distal extremities and fine hand and finger movements, it follows that the preservation of these fibers has been linked with good recovery post-stroke (Groisser *et al.*, 2014). More specifically, work done by Stinear and colleagues demonstrates that the functional potential in patients who do not exhibit motor evoked potentials following stroke declines as a function of corticospinal tract interruption (Stinear *et al.*, 2007). While many studies show that ipsilesional corticospinal tract integrity and volume are crucial components in determining recovery potential, they alone do not fully explain the emergence of abnormal joint coupling post-stroke.

Neural Reorganization Post-stroke

Contralesional neural activity

A healthy brain will show functional activity in motor cortex contralateral to a moving limb, but when the system becomes damaged, evidence suggests that contralesional sensorimotor cortex (that opposite the lesioned hemisphere) becomes more active during movement of the paretic limb. FMRI studies, measuring BOLD signals during movement, have found task-related activation in contralesional (ipsilateral to the paretic limb) M1 in stroke subjects (Calautti & Baron, 2003). During movement of the affected hand, those with greater clinical impairment showed a stronger influence from contralesional premotor cortex (Bestmann *et al.*, 2010), and overall patients with poorer outcomes tended to activate the unaffected hemisphere's cortical motor regions more than those with better outcomes (Johansen-Berg *et al.*, 2002). This shift towards contralesional activity is directly related to shoulder abduction load level in the paretic limb (Chen, 2007), suggesting a dynamic, use-dependent reliance on contralesional cortices post-stroke. Although the contribution of contralesional motor regions has been observed in many studies, it still remains unclear what neural substrates allow these regions to affect motor control output after a stroke.

The Brainstem Hypothesis

One explanation for why this contralesional shift occurs post-stroke is that after permanent damage to the descending corticofugal pathways, including the corticospinal tract, there may be a need for increased reliance on descending brainstem pathways (shown in green in Figure 2.3) to compensate. The brainstem hypothesis suggests that damaged corticospinal pathways provide inadequate drive to the paretic limb during increased shoulder abduction loading, requiring the system to rely more heavily on contralesional cortex to access bulbospinal

pathways. More specifically, anatomical and neurophysiological evidence suggests that the reticulospinal tract may have the potential to become more heavily relied upon post-stroke.

Reticulospinal Tract

Studies in primates show that the reticulospinal tract makes mono- and di-synaptic connections to motoneurons controlling muscles of the forearm (Riddle *et al.*, 2009). Stuart Baker and his colleagues went on to show that interneurons involved in controlling the hand often received convergent information from both corticospinal and reticulospinal projections (Riddle & Baker, 2010). Furthermore, EPSPs are present in hand muscles following stimulation of the medial longitudinal fasciculus, composed mainly of reticulospinal projections, although the magnitude of the EPSPs is much smaller compared to those generated by the CST (Baker, 2011). This evidence supports a potential role for the reticulospinal tract in control of the forearm and sheds light on its potential ability to help compensate after corticospinal tract damage.

Additionally, stimulation at the origin of the tract, the ponto-medullary reticular formation (PMRF), produces wrist flexor, elbow flexor and shoulder abductor activation, reflecting the tract's ability to simultaneously influence multiple motoneurons and to elicit the same movement patterns as those observed post-stroke. Further support comes from evidence that suggests that following a corticospinal tract lesion in primates, the connections from the medial longitudinal fasciculus undergo functional changes characterized by selective strengthening of inputs to forearm flexor and intrinsic hand motor neurons (Zaaimi *et al.*, 2012). If the corticospinal tract is damaged, the reticulospinal tract may possess the anatomical and physiological properties required to help drive motoneurons and interneurons controlling the forearm in the spinal cord. This evidence supports the hypothesis that the reticulospinal tract is a

strong potential candidate underlying abnormal joint coupling post-stroke. However, this has not been directly demonstrated in humans.

Robotic Approaches to Quantify Impairment

Impairment after stroke is commonly measured using clinical metrics such as the Fugl-Meyer Assessment, a performance-based index, which measures loss of independent joint function, stretch reflex hyper-excitability, and altered sensation (Fugl-Meyer *et al.*, 1975) (see a complete testing protocol in Appendix). Although the Fugl-Meyer Assessment is one of the most widely used clinical scales of motor impairment post-stroke (Gladstone *et al.*, 2002), it is determined through subjective, observational analysis on an ordinal scale, which does not account for the complex nature of some motor impairments. For example, expression of flexion synergy has been shown to be task dependent (Beer *et al.*, 1999; Dewald & Beer, 2001; Ellis *et al.*, 2007) and dynamic (Beer *et al.*, 2004; Sukal *et al.*, 2007; Ellis *et al.*, 2008). The more an individual attempts to drive the limb, the greater the activation of the flexion pattern and the lesser the ability to move outside of this pattern (Ellis *et al.*, 2016). This is a subtle feature that is not taken into account when using the Fugl-Meyer Assessment alone.

The use of robotics offers a task-dependent and dynamic way to better quantify the impact of flexion synergy on arm movement and even individual joints. A device that is capable of progressively manipulating proximal joint requirements can provide high-resolution information about the effects of loss of independent joint control. Using this approach, it becomes possible to quantify how the reaching range of motion (work area) (Sukal *et al.*, 2007) and hand opening (Lan, 2017) decreases as a function of increased abduction load on the shoulder after stroke. Ultimately, high-resolution measurements of specific impairments after

stroke will aid in determining the specific underlying mechanisms of deficits such as a loss of independent joint control. In the future, this approach could help in targeting motor impairments and in tracking recovery (Ellis *et al.*, 2016).

Overview of Neuroimaging Techniques

Magnetic resonance imaging (MRI) is a medical imaging technique based on the use of strong magnetic fields, radio waves and field gradients, used to generate images of the brain in health and disease.

T_1: Gray matter density

A T_1-weighted image is one of the basic pulse sequences used in MRI. T_1 is the longitudinal relaxation time, which represents the rate at which excited protons return to equilibrium. A T_1-weighted image produces contrast and brightness based on differences in the specific T_1 longitudinal relaxation time in various tissue types: white matter, gray matter, cerebrospinal fluid. Different tissue types have different T_1 values because the relaxation involves protons losing their excess energy via interactions with oscillating magnetic fields, which are produced by the magnetic moments of nuclei in surrounding tissue. Molecules in more viscous, lower mobility environments, such as those in neural gray matter, exhibit lower motional frequencies, producing magnetic fields that fluctuate at lower frequencies. In contrast, molecules in mobile liquids, such as those in cerebrospinal fluid, produce fluctuating magnetic fields over a much larger frequency range (Webb, 2003).

These differential tissue properties can help characterize pathological neural changes, such as degenerative loss and/or plastic reorganization, following a stroke-induced lesion. In order to assess gray matter across large groups of subjects, automated techniques such as voxel-

based morphometry (VBM) can be used (Whitwell, 2009). This technique uses T_1-weighted volumetric MRI scans to perform statistical tests across all voxels in multiple subjects to determine volumetric group differences (Ashburner & Friston, 2000).

More specifically, a VBM analysis begins by creating a study-specific brain template and segmentation of the image into individual tissue types based on the varying T_1 relaxation times in those different tissue types. The brains are extracted so that scalp tissue is removed from the image. T_1 images from each subject are then registered to a standard brain template and smoothed. Finally, a voxel-wise comparison and statistical testing are performed across all subjects. Statistical analysis is carried out on these maps using permutation testing and threshold-free cluster enhancement. VBM analysis can be used to compare gray matter density differences between groups (stroke vs. control) or to detect neuroanatomical correlates of behavioral deficits, such as loss of independent joint control.

Diffusion Imaging: White matter microstructure

Diffusion weighted MRI (Johansen-Berg & Behrens, 2014) is a powerful imaging technique that is currently the only method capable of mapping neural fiber architecture in vivo and non-invasively. It measures the dephasing of spins of protons in the presence of a spatially-varying magnetic field ('gradient') (Jones *et al.*, 2013), which can describe diffusion of water in biological tissues. Diffusion tensor imaging (Basser *et al.*, 1994) is one analysis technique of diffusion weighted MRI, which characterizes the magnitude, directionality (anisotropy), and orientation of water diffusion. This approach can detect subtle structural changes in tissue architecture that occur during pathologic processes of the central nervous system.

Water diffusion in biological tissues occurs inside, outside, around, and through cellular structures, to varying degrees. In white matter tissue, water diffusion is less hindered in the direction of fiber orientation but highly restricted in the direction perpendicular to the fibers. This feature gives water diffusion within white matter directionality, also called anisotropy, depending on the axonal orientation, and explains why diffusion tensor imaging is optimally suited to characterize white matter microstructure.

Measures of parallel and perpendicular diffusion within a given voxel can be modeled in a diffusion tensor and visualized using an ellipsoid: the eigenvectors representing the directions of the principle axes and the radii representing the apparent diffusivity strength (Alexander *et al.*, 2007). The primary eigenvector and eigenvalue (λ_1) describe the primary diffusion direction and magnitude, also called axial diffusivity (AD); the remaining eigenvalues (λ_2 and λ_3) can be averaged to describe diffusion perpendicular to the primary direction, also called radial diffusivity (RD). Fractional anisotropy (FA), a scalar value from 0 to 1, describes how directional the tensor model is in any given voxel and is a frequently used metric in diffusion imaging research in humans (equation below).

$$FA = \sqrt{\frac{(\lambda_1-\lambda_2)^2+(\lambda_2-\lambda_3)^2+(\lambda_1-\lambda_3)^2}{2(\lambda_1{}^2+\lambda_2{}^2+\lambda_3{}^2)}}$$

Each voxel in the brain can be described by this ellipsoid model and color-coded maps can be produced. These color maps represent left/right direction in red, anterior/posterior

direction in green and superior/inferior in blue. Figure 2.4 demonstrates the process by which

the measurement of water diffusion can create color-coded maps of the human brain in vivo.

In order to assess white matter microstructural integrity across large groups of subjects, a

technique such as tract-based spatial statistics (TBSS) can be used (Smith *et al.*, 2006). First, the

data get brain extracted, denoised, and corrected for motion and eddy currents. Each voxel in this

preprocessed diffusion-weighted image is then fit with a tensor model, which characterizes water
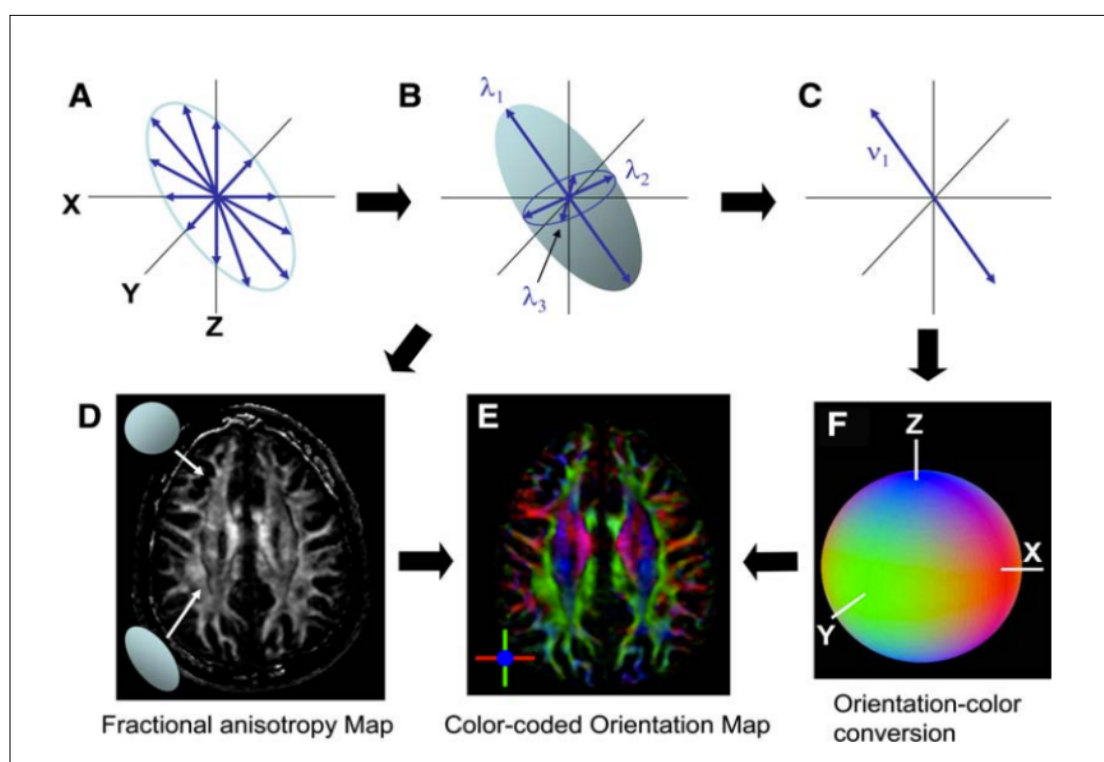
Figure 2.4
The Principle of DTI and Contrast Generation:
From diffusion measurements along multiple axes (A), the shape and the orientation of a "diffusion ellipsoid" is estimated (B). An anisotropy map (D) can be created from the shape, in which dark regions are isotropic (spherical) and bright regions are anisotropic (elongated). From the estimated ellipsoid (B), the orientation of the longest axis can be found (C), which is assumed to represent the local fiber orientation. This orientation information is converted to a color (F) at each pixel. By combining the intensity of the anisotropy map (D) and color (F), a color-coded orientation map is created (E) (Mori & Zhang, 2006).

diffusion directionality. Each resulting FA map gets registered to a standard space template, the Montreal Neurological Institute's (MNI) standard brain. A mean FA image is generated from all individual FA maps and used to create a common group skeleton, which represents the centers of all fiber bundles that are common to all subjects. A threshold is applied to minimize potential white matter/gray matter partial volume effects. Each subject's FA map is then projected onto the mean FA skeleton so that each skeleton voxel takes the FA value from the local center of the nearest relevant tract, addressing the issue of alignment (www.fmrib.ox.ac.uk/fsl). Finally, voxel-wise statistics are run to compare groups or obtain neuroanatomical correlates of behavioral deficits. Statistical analysis is carried out on these maps using permutation testing and threshold-free cluster enhancement.

This approach is simple to apply, can investigate the whole brain and does not require pre-specifying regions of interest. It is a more data-driven approach that can identify subtle changes in white matter microstructure, which may have previously been overlooked with purely hypothesis driven approaches.

Resting state functional connectivity

Functional magnetic resonance imaging is a safe, noninvasive technique that uses strong magnetic fields and magnetic gradients to record signals that, through appropriate processing and interpretation, can serve as a useful proxy for neural activity in a working and actively changing human brain. This technique has excellent spatial resolution, but suffers from poor temporal resolution.

The magnetic resonance signal depends on varying levels of deoxygenated hemoglobin in the blood (Ogawa *et al.*, 1990; Ogawa *et al.*, 1993). In order to produce energy, neurons require a sustained presence of oxygen, which travels through the blood bound to hemoglobin, a specialized protein. Neuronal activity alters the relative levels of oxygenated hemoglobin and deoxygenated hemoglobin, which causes the magnetic resonance signal to change. This signal change serves as the foundation for the blood oxygenation level-dependent (BOLD) signal measured in fMRI. It is important to note that the BOLD signal represents an indirect measure of metabolism, cerebral blood flow, and cerebral blood volume, and although proportional to levels of neural activity (Logothetis & Pfeuffer, 2004), should not be construed as a direct measure of neural activity (Lotze *et al.*, 2003).

There is important information present in the BOLD signals obtained at rest (Raichle, 2001; Raichle *et al.*, 2001). Spontaneous, low-frequency BOLD signal correlations between distinct regions at rest, known as resting state functional connectivity (rsFC), provide insight into the functional organization of the brain and can reflect networks that are active during a task (Biswal *et al.*, 1995). Resting state functional connectivity can serve as a useful tool for characterizing patient populations and quantifying neural changes in response to clinical interventions (Baliki *et al.*, 2012; Mutso *et al.*, 2014).

One common technique used is seed-based functional connectivity analysis. This method involves selecting a region of interest and correlating the average BOLD signal within this region (or seed) with the BOLD signal from every other voxel in the brain. The data undergo correction for motion, bandpass filtering to obtain only low frequency signals, and spatial smoothing. Signals from cerebrospinal fluid and white matter are regressed out, and scans are registered into

a standard space using the T_1 scan. The average time-course from voxels within the chosen seed are extracted and put in a correlation analysis with the time-course from all other voxels in the brain. Pearson correlation coefficient maps are produced and converted to z-values using Fisher's correction to improve normality. Statistical analysis is carried out on these maps using permutation testing and threshold-free cluster enhancement. This statistical testing can compare rsFC values between groups (stroke vs. control) or identify specific neuroanatomical functional correlates of impairment in patient populations.

Seed-based analysis can provide a precise and detailed look at the connectivity (or lack thereof) between brain areas of interest (Margulies *et al.*, 2007). This approach is advantageous in a patient population because it can include subjects that may not be able to perform a specific task, and it greatly diminishes the risk of motion artifacts that can emerge during a task-based fMRI scan.

Summary

The present review has provided an overview of stroke and a main impairment that develops as a consequence: loss of independent joint control. The aim of this work is to use an interdisciplinary approach combining robotics and multi-modal neuroimaging techniques to explore the underlying neural mechanisms behind this debilitating impairment. Understanding the neural substrates that contribute to a loss of independent joint control would help design more targeted interventions aimed at preventing or diminishing its effects after stroke.

3. Upper Extremity Motor Impairments and Microstructural Changes in Bulbospinal Pathways in Chronic Hemiparetic Stroke

Abstract

Following hemiparetic stroke, precise, individuated control of single joints is often replaced by highly stereotyped patterns of multi-joint movement, or abnormal limb synergies, which can negatively impact functional use of the paretic arm. One hypothesis for the expression of these synergies is an increased dependence on bulbospinal pathways such as the rubrospinal and especially the reticulospinal tracts, which coactivate multiple muscles of the shoulder, elbow, wrist and fingers. Despite indirect evidence supporting this hypothesis in humans post-stroke, it still remains unclear whether it is correct. We used high-resolution diffusion tensor imaging to quantify white matter microstructure in relation to severity of arm synergy and hand related motor impairments. Diffusion tensor imaging was performed on 19 moderately to severely impaired chronic stroke individuals and 15 healthy, age-matched controls. In stroke individuals compared to controls, there was significantly decreased fractional anisotropy and significantly increased axial and radial diffusivity in bilateral corona radiata and body of the corpus callosum. Furthermore, post-stroke the contralesional reticulospinal tract fractional anisotropy correlated significantly with both upper extremity synergy severity (r=-0.606, p=0.003) and hand impairment (r=-0.609, p=0.003). Fractional anisotropy in the ipsilesional rubrospinal tract significantly correlated with hand impairment severity (r=-0.590, p=0.004). For the first time, we

separately evaluate reticulospinal and rubrospinal tract microstructure in chronic stroke individuals with upper extremity motor impairment. We demonstrate that individuals with the greatest upper extremity synergy severity and hand impairments post-stroke have the highest fractional anisotropy in the contralesional reticulospinal tract, a pattern consistent with increased myelination and suggestive of neuroplastic reorganization. Since the reticulospinal pathway microstructure, in particular, is sensitive to abnormal joint coupling and hand related motor impairment in chronic stroke, it could help test the effects of specific, and novel, anti-synergy neurorehabilitation interventions for recovery from hemiparesis.

Introduction

Approximately 85% of stroke survivors experience significant motor impairment in the contralesional arm (Feys *et al.*, 1998), which can include a loss of independent joint control (Beer *et al.*, 2000; Miller & Dewald, 2012), weakness (Canning *et al.*, 2004), and spasticity (Opheim *et al.*, 2014). After stroke, precise, individuated control of single joints is often replaced by highly stereotyped patterns of multi-joint movement caused by abnormal muscle co-activation patterns (Dewald *et al.*, 1995). The most prevalent of these patterns is the flexion synergy, which is characterized by an abnormal coupling of shoulder abduction and elbow, wrist and finger flexion (Twitchell, 1951; Brunnstrom, 1970). This impairment has a negative impact on reaching ability (Ellis *et al.*, 2011) and hand function (Miller & Dewald, 2012; Lan, 2017), both critical components of functional use of the arm during activities of daily living. Despite the debilitating nature of this motor impairment, the underlying neuropathophysiology is not fully understood.

One hypothesis for why the flexion synergy emerges is that following a reduction of corticofugal input from the lesioned hemisphere, there is an increased dependence on

contralesional motor cortex and bulbospinal pathways such as reticulospinal (RetST) and rubrospinal tracts (RubST). Therefore, in the present study, we quantify microstructural properties in white matter of both the brain and the brainstem, focusing primarily on cortico-reticulospinal and cortico-rubrospinal systems. We evaluate whether these microstructural properties increase in integrity in relation to arm synergy and hand impairment severity, which could be indicative of increased use.

Although the RetST was previously believed to be predominantly involved in gross movements such as locomotion (Drew *et al.*, 1986; Matsuyama & Drew, 2000) and posture (Prentice & Drew, 2001; Schepens & Drew, 2004), recent work in primates suggests the RetST also influences the motor neurons that control forearm and intrinsic hand muscles (Riddle *et al.*, 2009). In the non-human primate, stimulation of the RetST produces ipsilateral wrist flexor, elbow flexor and shoulder abductor activation (Davidson & Buford, 2006), mirroring the flexion synergy pattern observed in humans post-stroke. Furthermore, stimulating the RetST after a corticospinal tract (CST) lesion elicits increased excitatory post-synaptic potentials in motoneurons innervating the forearm flexor and intrinsic hand muscles (Zaaimi *et al.*, 2012). This evidence makes the ispilateral (contralesional) cortico-reticulospinal system a compelling candidate for underlying abnormal joint coupling in humans with hemiparetic stroke.

In the non-human primate, the RubST also contributes to reaching and grasping movements (Kennedy *et al.*, 1986), and has been shown to be important in recovery of hand function after CST damage (Lawrence & Kuypers, 1968b; Belhaj-Saif & Cheney, 2000). One study showed that increased white matter integrity in bilateral red nucleus correlated with worse clinical outcomes in humans with chronic stroke (Ruber *et al.*, 2012); however, the RubST has

been reported as relatively insignificant in humans (Nathan & Smith, 1955; Onodera & Hicks, 2010). The evidence for whether the RetST and the RubST contribute to abnormal joint coupling and hand impairment in humans post-stroke still remains indirect and inconclusive.

We used high-resolution DTI (Basser *et al.*, 1994) tract-based spatial statistics (TBSS) (Smith *et al.*, 2006) to perform a voxel-wise comparison of white matter microstructure between stroke and control individuals. We analyzed fractional anisotropy (FA), a measurement typically associated with tract integrity, as well as axial (AD) and radial diffusivity (RD), which represent diffusion parallel and perpendicular to the principle direction of diffusion, respectively. Because previous studies have reported altered diffusion properties in lesioned tissue (Stinear *et al.*, 2007; Jason *et al.*, 2011; Puig *et al.*, 2013), we excluded potential lesion-compromised voxels from our TBSS analysis to assess changes in normal appearing white matter. We used the TBSS-derived white matter skeleton to investigate whether microstructural tissue properties within specific regions of the brainstem (CST, RetST, RubST) and subcortical white matter within contralesional motor areas (M1, PM, SMA, body of the Corpus Callosum) are sensitive to upper extremity motor impairment in chronic stroke individuals.

We evaluated upper extremity motor impairment using the Fugl-Meyer Assessment (FMA), a stroke-specific, performance-based motor impairment index, which measures impairments such as loss of independent joint function, stretch reflex hyper-excitability and altered sensation (Fugl-Meyer *et al.*, 1975). It is one of the most widely used clinical scales of motor impairment post-stroke (Gladstone *et al.*, 2002). While previous studies have looked at diffusion MRI metrics in relation to the entire FMA score (Takenobu *et al.*, 2014; Li *et al.*, 2015), we used only the upper extremity measurements of arm synergies and hand function to

determine whether microstructural properties in specific white matter regions of interest (ROIs) were correlated.

In the present study, we hypothesized that microstructural integrity in specific regions of the extrapyramidal brainstem would be increased in chronic stroke in a manner sensitive to synergy and hand related impairment severity. We demonstrate a significant decrease in fractional anisotropy in bilateral corona radiata and body of the corpus callosum in chronic stroke when compared to controls; however, within stroke subjects, specific brainstem regions show the highest FA in individuals with the most synergy-driven arm and hand impairment. More precisely, we describe the relation between contralesional RetST integrity and both expression of synergy and hand impairment and between ipsilesional RubST integrity and hand impairment in chronic hemiparetic stroke individuals.

Methods

Patients and healthy controls

19 moderately to severely impaired stroke individuals (15M,4F; average age 59 years, standard deviation 8 years; 9 severe, 10 moderate), and 15 age-matched healthy controls (8M,7F; average age 61 years, standard deviation 7 years) without known neurological abnormalities were included in the study. Stroke subjects sustained a unilateral brain lesion from a stroke at least four months prior to participation in the study. Stroke participants were selected from the Clinical Neuroscience Research Registry, housed in the Rehabilitation Institute of Chicago, as well as from individuals residing in Chicago who wished to participate.

Inclusion criteria for stroke individuals were as follows: 1) paresis confined to one side, with motor impairment of the upper limb, 2) an overall Upper Extremity FMA score between 0

and 50 out of 66 (0-20=severe, 21-50=moderate (Velozo & Woodbury, 2011)), 3) absence of severe cognitive or affective dysfunction, 4) absence of severe concurrent medical problems. The protocol was approved by the Northwestern University Institutional Review Board, and all subjects provided a written, informed consent in accordance with the Declaration of Helsinki. Table 3.1 shows the clinical characteristics of the stroke individuals.

Table 3.1
Patient demographics and clinical characteristics of all stroke subjects enrolled in the study.

	Age (years)	Time post stroke (months)	Lesioned hemi	Lesion location	UE-FMA total	FMA synergy	FMA hand
S01	61–65	237	R	IC, BG, Thal	11	9	2
S02	46–50	209	L	IC, BG, Thal	17	9	2
S03	61–65	82	R	IC, BG	14	10	0
S04	66–70	26	R	Par, Occ, IC	15	10	1
S05	71–75	160	R	IC	15	9	2
S06	61–65	359	L	IC, BG, Thal	16	10	2
S07	51–55	5	L	Par, IC	21	11	2
S08	66–70	246	L	IC, BG, Thal	17	12	1
S09	61–65	83	R	IC, Pons	17	11	3
S10	61–65	96	R	IC, BG	19	10	1
S11	56–60	100	R	Par, IC, BG, Thal	22	17	1
S12	56–60	138	R	Occ, IC	22	18	3
S13	61–65	90	L	IC	24	14	2
S14	66–70	95	L	Thal	29	14	6
S15	56–60	52	L	IC, BG	29	18	3
S16	35–40	106	R	Par, IC, Thal	29	17	5
S17	51–55	95	R	Occ, IC, Thal	36	22	6
S18	61–65	106	L	IC, Thal	32	19	7
S19	46–50	59	R	IC, BG, Thal	33	18	8

BG, basal ganglia; FMA, Fugl-Meyer assessment; IC, internal capsule; Occ, occipital lobe; Par, parietal lobe; Thal, thalamus; UE, upper extremity.

Clinical Assessment

Upper extremity Fugl-Meyer Assessment (FMA) was performed by a licensed physical therapist to evaluate motor impairment in stroke individuals. Higher values indicated less impairment (Fugl-Meyer *et al.*, 1975). From this assessment, arm synergies (range: 9 to 22 out of a maximum score of 30) and hand related impairments (range: 0 to 8 out of a maximum score of

24) were calculated separately. In our subsequent analysis, we determined which neural regions were correlated to synergy related arm impairment or hand impairment.

Data Acquisition

MRI scans were performed at Northwestern University's Center for Translation Imaging on a 3 Tesla Siemens Prisma scanner with a 64-channel head coil. Structural T1-weighted scans were acquired using an MPRAGE sequence (TR=2.3s, TE=2.94ms, FOV=256x256mm^2) producing an isotropic voxel resolution of 1x1x1mm^3 and lasting 10 minutes. Diffusion weighted images were collected from all subjects using spin-echo echo-planar imaging (TR=5s, TW=85ms, matrix size=150x150, FOV=225x225mm, slice thickness=1.5mm, interslice gap=0mm, number of slices=120) producing an isotropic voxel resolution of 1.5x1.5x1.5mm^3 and lasting 5 minutes. The sequence consisted of diffusion weighting of 1000s/mm^2 in 60 different directions and 8 scans with no diffusion weighting (b=0s/mm^2). Visual inspection of acquired images was performed immediately following the data acquisition to guarantee no artifacts and stable head position.

DTI pre-processing

The diffusion-weighted images were first brain-extracted using the BET toolbox in FSL (http://www.fmrib.ox.ac.uk/fsl). The data were then denoised using an estimate of the noise variance in CSF signal intensity of the right ventricle (Aja-Fernandez *et al.*, 2008) and Rician noise corrected (Ingo *et al.*, 2014). The data were corrected for motion and eddy currents by co-registering diffusion weighted images to the image acquired with b=0s/mm^2 using the FLIRT

toolbox in FSL. The motion correction transformation matrix was applied to the diffusion gradient directions to rotate them according to the registration algorithm. The pre-processed diffusion weighted data were fitted to a tensor on a voxel-wise basis using DTIFIT in the FSL Diffusion Toolbox (Behrens *et al.*, 2003).

TBSS Analysis

For those individuals with lesions in the left hemisphere, FA maps were flipped so that all subjects had lesions in the right hemisphere and group analysis compared all contralesional hemispheres in the left hemisphere. FA maps were first linearly and then non-linearly registered to the FMRIB58_FA in Montreal Neurological Institute's (MNI) standard space. A mean FA image was then created from all individual FA images, and used to generate a common group skeleton. A threshold was applied at 0.2 to minimize potential white matter / gray matter partial volume effects. Finally, each FA image was projected onto the common group skeleton for subsequent statistical analysis. The same transformations were applied to both axial diffusivity (AD) and radial diffusivity (RD) maps, which represent diffusion parallel and perpendicular to the principal direction of diffusion, respectively.

Lesion mask

Lesion masks were generated on the T1-weighted scans using automated pipelines developed at Northwestern University (Wang *et al.*, 2015). For those individuals with lesions in the left hemisphere, lesion masks were flipped into the right hemisphere so that group analysis compared all contralesional hemispheres in the left hemisphere. For each subject, T1 images

were brain extracted and affine registered to the b=0s/mm^2 diffusion scan using FSL FLIRT (Jenkinson & Smith, 2001; Jenkinson *et al.*, 2002). The same transformation matrix was applied to align individual lesion masks to the subject specific diffusion image, with the assumption that hypointensity due to the lesion in the T1-weighted image matched the hyperintensity due to the lesion in the T2-weighted b=0s/mm^2 image. The lesion mask for each subject was transformed into MNI space, utilizing the same transform applied to the FA images. A cumulative right hemisphere lesion mask was created for all stroke individuals by adding individual lesion masks from each subject in standard space. This common lesion mask was used to exclude all lesioned voxels from subsequent TBSS analysis and to ensure statistical testing was performed only on normal appearing white matter, with regard to T1-weighted signal, in all subjects.

TBSS Statistical Analysis

In order to determine voxel-wise statistics between stroke subjects and healthy controls, permutation testing was applied to the 4D skeletonized FA, AD, and RD maps, with lesioned voxels excluded. Using RANDOMISE in FSL, 5000 permutations with threshold-free cluster enhancement were performed to correct for multiple comparisons (Winkler *et al.*, 2014).

ROI Analysis

A region of interest (ROI) analysis was performed using the TBSS-generated white matter skeleton to further quantify diffusion characteristics in a specific subset of neural regions relevant to motor recovery post-stroke. These included contralesional white matter from motor regions: primary motor (M1), premotor (PM), and supplementary motor area (SMA) and body of

the corpus callosum as shown in Figure 3.1A,B and bilateral brainstem regions, which included cerebral peduncles (CP), containing descending projections of the CST, reticular formation (RF) containing part of the descending RetST, and red nucleus (RN) containing descending RubST projections, shown in Figure 3.1 C-E. The cerebral peduncle and corpus callosum masks were obtained from the JHU ICBM-DTI-81 White-Matter Atlas (Mori, 2005; Wakana *et al.*, 2007; Hua *et al.*, 2008); the motor region masks were obtained from Human Motor Area Template (Mayka *et al.*, 2006); the RN and RF masks were drawn manually in the midbrain and pons based on known anatomy (Standring, 2016) and extended caudally to capture descending projections. The midbrain region was carefully selected because at this level, CP, RF and RN are visibly separable (Felton, 2003). Average FA values were calculated from all white matter skeleton voxels within each ROI: left CP, right CP, left RetST, right RetST, left RubST, right RubST, white matter from motor regions (M1, PM, SMA) and body of the corpus callosum.
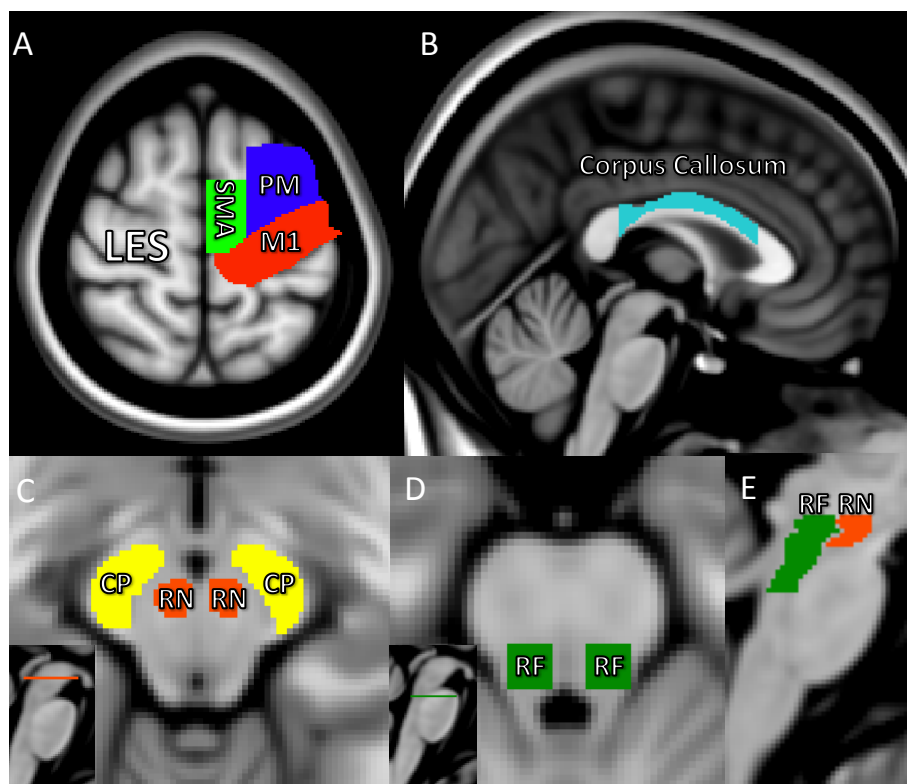
Figure 3.1
Region of interest masks in Montreal Neurological Institute's space. (A) Primary motor area (red), supplementary motor area (green), premotor area (blue), (B) body of the corpus callosum (light blue), (C) horizontal midbrain cross-section showing cerebral peduncle (CP) portion of the corticospinal tract (yellow) and red nucleus (RN) (red), (D) horizontal pontine cross-section showing reticular formation (RF) (green), and (E) sagittal brainstem showing RF including reticulospinal (green) and RN including rubrospinal tracts (red).

ROI Statistical Analysis

If an ROI did not show significant differences in TBSS, the stroke group was split into severe and moderate based on FMA score (0-20=severe, 21-50=moderate (Velozo & Woodbury, 2011)), for further analysis in which a one-way ANOVA and post-hoc testing were performed on the control, moderate stroke and severe stroke group ROI values. Furthermore, a Spearman correlation analysis was carried out between both hand and arm components of the UE-FMA and

average FA values within each ROI: left and right CP, left and right RetST and left and right

RubST, white matter from contralesional motor regions (M1, PM, SMA) and body of the corpus

callosum across stroke participants. If there was no significant correlation for FA and impairment

within an ROI, AD and RD were analyzed for possible correlation to impairment. For all non-

significant correlations between FA and impairment presented in Table 2, correlations for AD

and RD were also non-significant. We accounted for multiple comparisons using a Bonferroni

correction. An overall alpha-level of 0.005 was considered significant, which was obtained by

dividing alpha of 0.05 by the 10 comparisons that were made. There was a significant correlation

Table 3.2
r and p values for correlations between upper extremity FMA (synergy and hand) and fractional anisotropy values in specific brain regions.

	Synergy		Hand	
	r	*p*	*r*	*p*
Ipsilesional CP	−0.089	0.357	−0.132	0.295
Contralesional CP	−0.531	*0.010*	−0.520	*0.011*
Ipsilesional RetST	−0.159	0.257	−0.259	0.142
Contralesional RetST	−0.606	**0.003**	−0.609	**0.003**
Ipsilesional RubST	−0.282	0.121	−0.590	**0.004**
Contralesional RubST	−0.349	0.072	−0.386	0.051
Contralesional M1	−0.102	0.339	−0.140	0.284
Contralesional PM	−0.257	0.144	−0.015	0.475
Contralesional SMA	−0.415	*0.039*	−0.142	0.281
Corpus callosum	−0.502	*0.014*	−0.364	0.063

CP, cerebral peduncle; RetST, reticulospinal tract; RubST, rubrospinal tract; M1, primary motor tract; PM, premotor tract; SMA, supplementary motor tract.
Bold signifies reaching statistical significance of p < 0.005.
Bold-italic signifies trends such that 0.005 < p < 0.05.

between synergy and hand FMA components (r=0.642, p=0.0015).

Results

Lesion mask

Figure 3.2 shows the cumulative lesion mask for all stroke individuals. Areas that appear in yellow signify a higher number of subjects had a lesion in that voxel. Voxels in which at least one individual had a lesion were excluded for subsequent TBSS analysis.
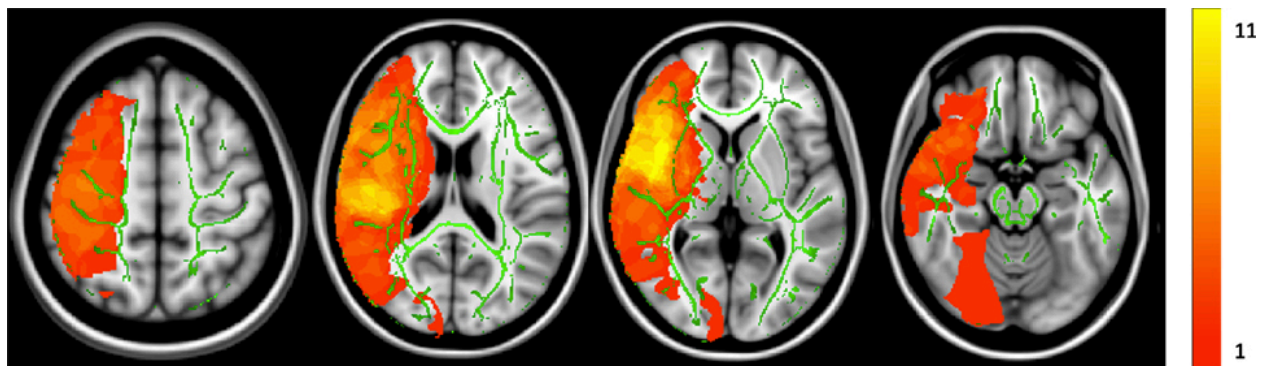
Figure 3.2
Cumulative lesion mask for all stroke subjects. Z=126, 90, 75 and 55. The color bar indicates how many subjects sustained a lesion in that particular voxel. The maximum was 11 subjects sharing a single-lesioned voxel with a minimum of one individual. The average group white matter skeleton is shown in green.

TBSS analysis stroke vs. control

Figure 3A-C shows the average group white matter skeleton in green, with lesion-compromised voxels removed in the right hemisphere. In Figure 3A, there is significantly decreased FA in regions of the corona radiata, corpus callosum and ipsilesional cerebral peduncle (CP) in stroke when compared to controls, shown in red. Figures 3B and 3C show there
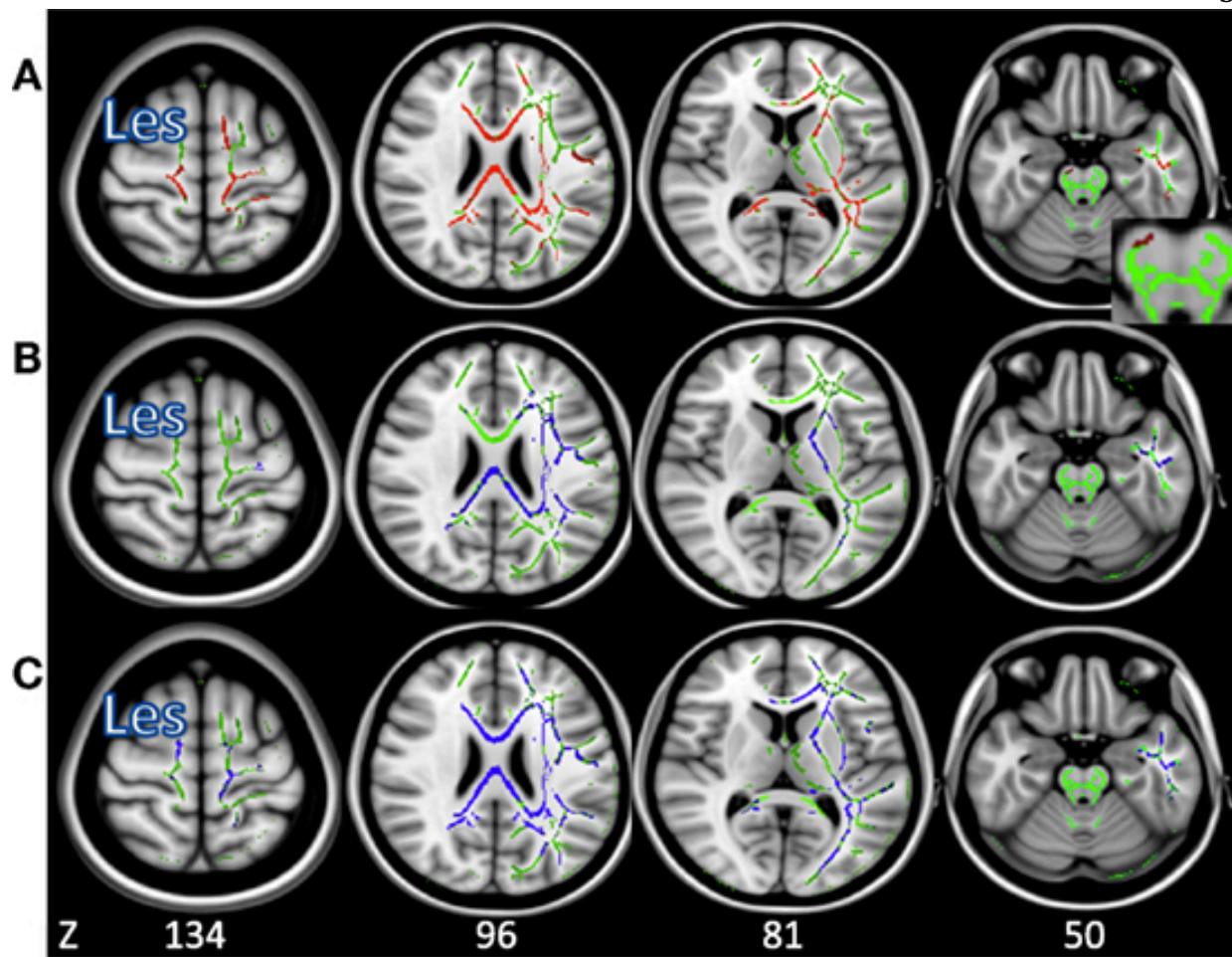
Figure 3.3
(A) Voxels in which fractional anisotropy is decreased in stroke compared to control (p < 0.05) shown in red. (B) Voxels in which axial diffusivity is increased in stroke compared to control (p < 0.05) shown in blue. (C) Voxels in which radial diffusivity is increased in stroke compared to control (p < 0.05) shown in blue. The average group skeleton is shown in green. Les signifies the lesioned hemisphere.

was significantly increased AD and RD in motor regions of the corona radiata, internal capsule and corpus callosum in stroke when compared to controls, shown in blue.

In contrast, the contralesional CP, bilateral RetST and bilateral RubST ROIs showed no significant group differences in the TBSS analysis, and were further analyzed by subdividing the stroke group. When dividing the stroke group into moderately (FMA 21-50) and severely

impaired (FMA 0-20) groups, there was no significant effect of group on the diffusion measures of the contralesional CP or bilateral RubST. However, there was a statistically significant difference between groups as determined by one-way ANOVA for FA in contralesional RetST (p=0.0063). Post-hoc testing revealed that FA in contralesional RetST was significantly higher in severely impaired individuals (0.41±0.03, p=0.0045) compared to moderately impaired individuals (0.36±0.02). This result was primarily driven by differences in RD (p=0.024) rather than AD (p=0.866). The average FA value for the control group (0.39±0.03) was between the average FA values of the moderately and severely impaired individuals, but statistical significance was not reached for these comparisons (severe vs. control (p=0.243), moderate vs. control (p=0.093)). These results are shown in Figure 3.4.
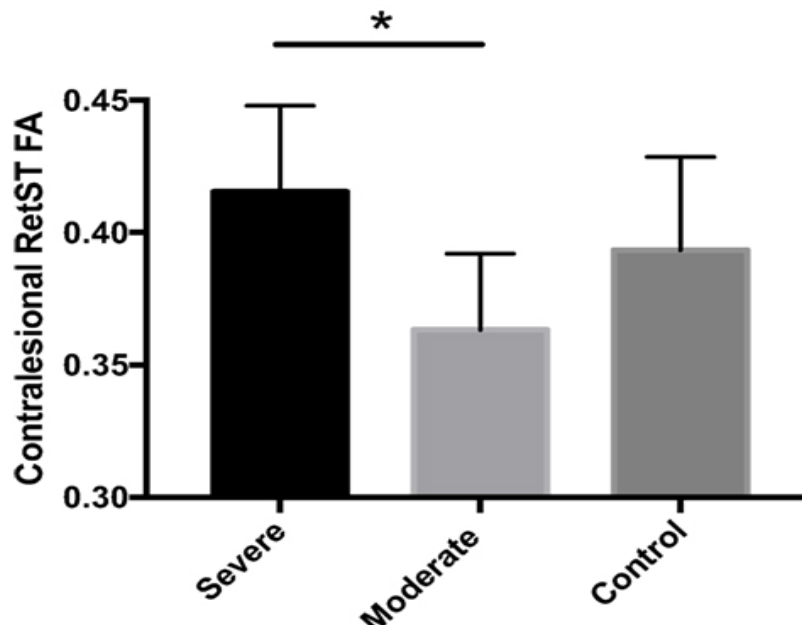
Figure 3.4
Average contralesional reticulospinal tract (RetST) fractional anisotropy (FA) for severe stroke group (0.415), moderate stroke group (0.363), and control group (0.393). Severely impaired individuals show significantly greater FA (p = 0.0045) than moderately impaired individuals. SD bars are shown. 95% confidence intervals were severe [0.39, 0.43], moderate [0.34, 0.38], and control [0.37, 0.41].

Correlation analysis within stroke

A correlation analysis was performed for the synergy and hand components of the upper extremity FMA and the ROIs thought to be involved in motor recovery, shown in Table 2. There were significant negative correlations between synergy expression in the arm and contralesional RetST (Figure 5A), indicating that individuals with the most synergy expression had the highest FA in this region. There was a trend of a negative correlation between synergy expression and FA of the contralesional CP, contralesional SMA white matter and body of the corpus callosum, and no significant correlations between synergy expression and FA of ipsilesional CP,

ipsilesional RetST, bilateral RubST, contralesional M1 or contralesional PM areas (Table 2).

There were no significant correlations between FA in ipsilesional M1, PM and SMA white matter and impairment severity. Additionally, since there was a significant correlation between synergy and hand FMA components, we cannot consider the results independent, but related as the significance patterns of correlations across brain regions demonstrate in Table 3.2.

There was a significant correlation between hand impairment scores and FA in contralesional RetST (Figure 5B) and ipsilesional RubST (Figure 5C). There was a trend of negative correlation between hand impairment and FA of the contralesional CP. No significant correlations were found between hand scores and FA in bilateral CP, ipsilesional RetST, contralesional RubST, contralesional M1, PM, SMA white matter, or corpus callosum.
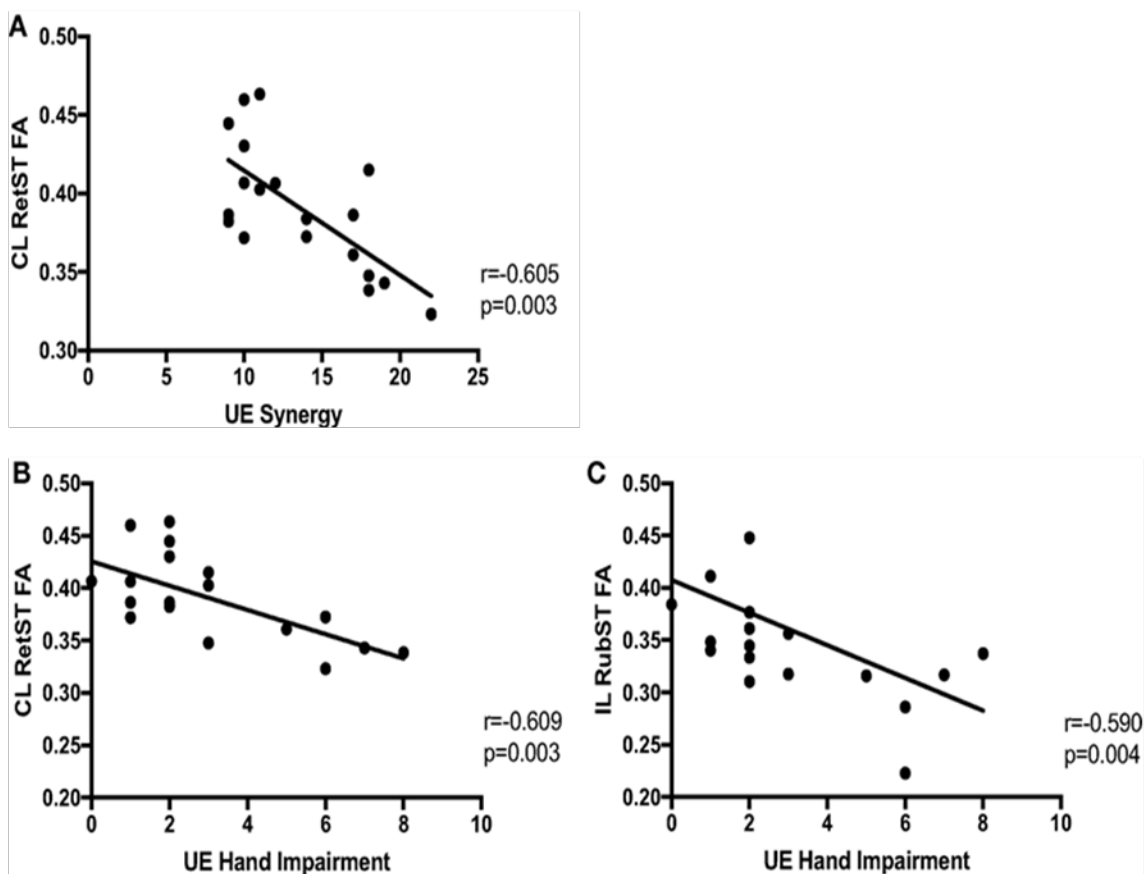
Figure 3.5
Correlations between impairment and brainstem white matter microstructure. Upper extremity (UE) synergy expression is correlated with **(A)** fractional anisotropy (FA) in contralesional (CL) reticulospinal tract (RetST) (95% CI [−0.83, −0.19]). UE hand impairment is correlated with **(B)** FA in CL RetST (95% CI [−0.83, −0.20]) and **(C)** FA in ipsilesional (IL) rubrospinal tract (RubST) (95% CI [−0.82, −0.17]).

Discussion

Summary of Results

Our results support previous reports of decreased FA and increased AD and RD in white matter of motor regions, corpus callosum and ipsilesional cerebral peduncle post-stroke compared to healthy controls (Lindenberg *et al.*, 2012; Li *et al.*, 2015), a pattern that reflects

chronic white matter degeneration. We extend these findings by showing that in chronic hemiparetic stroke, microstructure in the contralesional RetST was related to both synergy and hand impairment, and microstructure in the ipsilesional RubST was related to hand impairment. Individuals with the most severe synergy driven impairment had higher FA in contralesional RetST when compared to moderately impaired individuals, a pattern which reflects plastic remodeling in healthy controls (Scholz *et al.*, 2009). Our findings also show that the ipsilesional RubST may play a role in the expression of hand impairment in more impaired individuals with chronic stroke and emphasize the importance of including brainstem morphology into models of neural reorganization post-stroke.

Specific changes in brainstem white matter in chronic hemiparetic stroke

The contralesional RetST

Previous studies have used diffusion MRI to show that decreased FA in lesioned CST and corpus callosum are sensitive to impairment post-stroke (Chen & Schlaug, 2013; Li *et al.*, 2015). In the present study, we included the brainstem and identified a region in the contralesional RetST, which showed increased FA in the most severely impaired individuals (Figure 4), a difference primarily driven by a decrease in RD, shown to be related to myelination in animal models (Song *et al.*, 2003).

Impairment dependent differences within stroke have been described in previous studies. For example, in moderately impaired individuals, shoulder abduction reduced reaching distance and voluntary hand opening, but in severely impaired individuals performing the same task, while lifting the arm, reaching became almost impossible and grasping forces were generated at

the hand (Sukal *et al.*, 2007; Ellis *et al.*, 2016; Lan, 2017). This finding could be indicative of damage-dependent reorganization in the most severely impaired individuals, who may need to rely more heavily on contralesional RetST to elicit movement, albeit synergistic and dysfunctional in nature, post-stroke.

Initial work characterizing the RetST focused on its role in gross movements such as locomotion (Mori *et al.*, 2001), and postural stability (Schepens *et al.*, 2008); however, recent studies in primates show that the RetST makes mono- and di-synaptic connections to motor neurons controlling muscles of the forearm (Riddle *et al.*, 2009). Interneurons involved in controlling the hand often receive convergent information from both CST and RetST (Riddle & Baker, 2010), and stimulating the RetST elicits excitatory post-synaptic potentials in hand muscles (Baker, 2011). Historically, it has been assumed that the CST almost exclusively controls the hand, but anatomical evidence in primates suggests a more nuanced model of forearm and hand control in which RetST contributes less selective input, and CST provides much stronger, more fractionated and precise commands (Miller & Dewald, 2012).

Including the RetST contributions in our understanding of hand control could help inform what happens when there is significant stroke-related damage to the CST. Stimulation of the reticular formation in a non-human primate produces ipsilateral elbow, wrist and finger flexor and shoulder abductor activation (Davidson & Buford, 2006), reflecting the role of the RetST in simultaneously influencing multiple motor neurons and mirroring the flexion synergy pattern observed in humans post-stroke. Additionally, following a CST lesion in primates, RetST connections to both forearm and hand muscles selectively strengthen (Zaaimi *et al.*, 2012). If the CST is damaged, the contralesional corticoreticulospinal pathway may possess the properties

required to help drive motor neurons and interneurons controlling the forearm in the spinal cord, but this could come at the cost of independent control of individual joints. This anatomical and physiological evidence supports the hypothesis that the RetST is a potential pathway that could explain the development of the flexion synergy post-stroke.

The ipsilesional RubST

In non-human primates, the magnocellular subdivision of the red nucleus gives rise to the RubST, which decussates and descends down to the contralateral spinal cord. Cells in the red nucleus receive input from primary motor cortex (Humphrey *et al.*, 1984). In the absence of the CST, animals with a lesioned RubST lose the ability to grasp (Lawrence & Kuypers, 1968b), and output from the RubST has been shown to strengthen after unilateral CST lesion (Belhaj-Saif & Cheney, 2000). Despite this evidence from non-human primates, it has been argued that humans do not have a significant RubST descending from the midbrain (Nathan & Smith, 1955); however, a new tractography study has been able to trace this pathway *in vivo* (Meola *et al.*, 2016). Other recent DTI studies in human stroke individuals show a gradual increase in FA in ipsilesional red nucleus during stroke recovery (Takenobu *et al.*, 2014), and increased FA bilaterally in red nucleus when compared to controls, which is correlated with worse clinical outcomes (Ruber *et al.*, 2012). We build on these findings by demonstrating that microstructural integrity of the ipsilesional RubST is significantly related to hand impairment. This is anatomically consistent with animal evidence, which supports a role for RubST in contralateral hand-grip. Following a loss of CST, the RubST may provide an additional means to preserve finger flexion, particularly for individuals with the most severe upper extremity impairments.

Additional regions sensitive to motor impairment post-stroke

We observed a trend of negative correlations between upper extremity synergy expression and FA in contralesional CP, corpus callosum, and white matter projections from contralesional SMA. Non-human primate work has demonstrated that, of the three cortical motor areas (M1, PM, SMA), direct stimulation of premotor regions (PM, SMA) can result in ipsilateral activity in proximal muscles of the upper extremity, with significantly more responses following SMA stimulation (Montgomery *et al.*, 2013). The latency of these responses suggested that they were more likely to be polysynaptic, and anterograde tracers showed a direct projection from SMA to labeled reticulospinal cells (Montgomery, 2013). TMS studies support the presence of upregulated polysynaptic pathways ipsilateral to the paretic limb in humans post-stroke (Schwerin *et al.*, 2008; Schwerin *et al.*, 2011). The contralesional corticoreticulospinal pathway may serve as an alternative, indirect route to access motoneurons post-stroke, particularly in the most severely impaired individuals; however, our results suggest that white matter diffusion properties in SMA are not as sensitive to impairment severity as diffusion properties in the brainstem.

Surprisingly, FA of the ipsilesional cerebral peduncle, containing the CST, was not sensitive to either arm synergy or hand related impairment. However, there has not been an established consensus in previous works regarding the ipsilesional CST and impairment severity (Stinear *et al.*, 2007; Schaechter *et al.*, 2009; Globas *et al.*, 2011; Qiu *et al.*, 2011; Borich *et al.*, 2012; Song *et al.*, 2012; Chen & Schlaug, 2013; Puig *et al.*, 2013). Some studies tested whether FA values along the CST relate to functional recovery during an intervention (Stinear *et al.*, 2007; Globas *et al.*, 2011; Lindenberg *et al.*, 2012; Puig *et al.*, 2013). In contrast, our study

focused on moderately to severely impaired chronic individuals and synergy severity in the upper limb. Another study showed that greater FA asymmetry in the internal capsule was associated with poorer upper limb function, but only for individuals who did not demonstrate motor evoked potentials (MEPs) using transcranial magnetic stimulation. In patients with MEPs, FA asymmetry had no predictive power for clinical score (Stinear *et al.*, 2007), showing the relation to FA asymmetry was only present in a subset of patients studied. Another study found an insignificant trend between FA in the CST and baseline motor deficits, and these values did not predict the response to unilateral arm training (Globas *et al.*, 2011).

Some studies have shown a relationship between FA of the CST and motor skill in chronic stroke (Schaechter *et al.*, 2009; Qiu *et al.*, 2011). These studies had key differences such as using a clinical test that measures finger function (Schaechter *et al.*, 2009), including lesioned voxels (Qiu *et al.*, 2011), and focusing on individuals with good recovery (Wen *et al.*, 2016). However, a number of studies support our findings, in that they did not find any significant relationship between FA in the ipsilesional CST and motor impairment (Borich *et al.*, 2012; Song *et al.*, 2012; Chen & Schlaug, 2013). The exact role of microstructural status of the ipsilesional CST plays in long-term impairment in chronic stroke individuals remains unclear. This further emphasizes the importance of understanding the role of all descending motor pathways in relation to recovery, or lack thereof, after stroke.

Interpreting diffusion property changes

FA is sensitive to neural microstructural architecture, but cannot identify the precise biological sources of diffusion changes. By including other diffusion metrics, such as AD and

RD, we can more specifically describe observed microstructural changes in vivo. Animal models have suggested that AD may be sensitive to axonal damage, whereas RD has been linked to myelin integrity (Song *et al.*, 2003). A recent study showed that FA was significantly correlated with myelin basic protein, suggesting that FA is also highly sensitive to myelination (Chang *et al.*, 2017b).

In stroke when compared to control, we found decreased FA—driven by increases in AD and RD—in bilateral motor regions, body of the corpus callosum, and ipsilesional cerebral peduncle, which could be reflective of chronic degenerative changes (Concha *et al.*, 2006); however, a decrease in FA after training has also been reported (Wan *et al.*, 2014). Because we removed lesioned voxels from our TBSS analysis, we can be more confident that these results are reflective of changes in non-lesioned tissue, indicating that microstructure is altered even in normal appearing white matter. Since the majority of our participants sustained their strokes years, or even decades prior to the study, our findings demonstrate that these widespread microstructural changes are maintained long-term.

In contrast to the widespread decrease in FA, we identified a region in the extrapyramidal brainstem which shows increased FA in the most severely impaired individuals. This increase in FA was primarily driven by a decrease in RD, with AD showing no significant between-group difference, suggesting that the change could be myelin driven. This finding may be indicative of neuroplastic reorganization in individuals who rely more heavily on brainstem pathways to elicit movement post-stroke.

Limitations

Following stroke, impairment of motor function is one of the most serious consequences. Thus, we need better tools that can help us predict motor impairment in the paretic limb, such as more quantitative peripheral measurements of impairment. In addition, although we have carefully tried to identify and isolate specific pathways, the brainstem contains complex architecture and tightly packed structures. The crus cerebri of the cerebral peduncle contain corticobulbar pathways and pontine projections, and the dorsal pons includes other pathways such as the tectospinal tract. Future work will combine more quantitative metrics of impairment with higher resolution brainstem imaging, and include stroke groups with and without synergy expression to further elucidate the mechanisms underlying abnormal joint torque coupling post-stroke.

Conclusion

Our findings demonstrate that different neural regions may serve as potential backup systems, depending on the level of motor impairment post-stroke. Previous studies, using diffusion MRI, have focused on the role that the CST and the corpus callosum play in recovery, but the microstructural properties of brainstem motor pathways, specifically the corticoreticulospinal and corticorubrospinal systems, have not been studied separately *in vivo* in chronic hemiparetic stroke. Our results highlight the importance of including the brainstem motor pathways in models of neural reorganization. They provide potential new research-relevant biomarkers, which are sensitive to synergy and hand related motor impairments in chronic hemiparetic stroke. Higher resolution diffusion imaging and detailed atlases will be instrumental in better defining the basic anatomy and connectivity of the human brainstem and determining how it is affected by neural injury. Our study demonstrates the complex,

heterogeneous patterns of morphological neural changes as a function of motor impairment level, and emphasizes the need for understanding which systems are spared or reorganized after stroke. The current findings provide a framework for the future exploration of the effect of anti-synergy interventions (Ellis *et al.*, 2009a; Ellis *et al.*, 2009b) that may promote the maximal utilization of spared corticospinal resources in the lesioned hemisphere. This may lead to largely avoiding or reversing structural and functional changes to indirect contralesional motor pathways, thus minimizing the devastating effects of the flexion synergy on functional use of the paretic arm after stroke.

4. Changes in Structural and Functional Properties in Contralesional Corticobulbospinal Pathways in Chronic, Hemiparetic Stroke

Abstract

Our previous work used diffusion imaging to demonstrate that white matter microstructure in contralesional reticulospinal pathways is altered in severely impaired stroke individuals when compared with moderately impaired stroke individuals and controls. Here we aimed to determine whether functional connectivity during rest and cortical gray matter density changes were also present in chronic stroke individuals. We find that resting state functional connectivity between the contralesional brainstem and contralesional motor cortex is increased in chronic, hemiparetic stroke. Additionally, we find that gray matter density in contralesional motor cortex and white matter microstructure in contralesional corticofugal pathways is increased in the most severely impaired individuals. We therefore provide evidence for structural and functional reorganizational changes after stroke-induced neural damage, specifically in contralesional corticoreticulospinal pathways in the most severely impaired individuals.

Introduction

Neural plasticity in sensorimotor cortical regions and remaining corticospinal fibers have been the primary focus of neuroimaging research following damage to neural circuitry, as in the case of a unilateral brain injury such as stroke. In contrast, neuroplastic changes at the level of the brainstem, more specifically the bulbospinal pathways, have only received limited attention. Previous work indicates that white matter changes in the brainstem may be a sensitive biomarker

of neural plasticity following unilateral brain injury (Owen *et al.*, 2017). Therefore, we expand on this idea by exploring how brainstem motor pathways are functionally connected with the cortex by non-invasively studying the structural and functional characteristics of contralesional corticobulbospinal pathways in chronic hemiparetic stroke.

After stroke, the brain can compensate for neural tissue damage by reorganizing its surviving networks, a process that has been linked to degree of functional recovery. Specifically, neuroimaging studies have shown that after stroke, movements of the affected limb are associated with increased neural activity in both the lesioned and non-lesioned hemisphere (Ward *et al.*, 2003a; Grefkes *et al.*, 2008), with poorly recovered individuals more likely to recruit contralesional motor cortex (Ward *et al.*, 2003b; Calautti *et al.*, 2007). Despite robust evidence of increased contralesional neural activity during movement post-stroke (Rehme *et al.*, 2012), it remains unclear precisely how this contralesional cortical activity contributes to functional use of the paretic upper limb. One hypothesis is that following a reduction of corticofugal input from the lesioned hemisphere, there is increased dependence on contralesional motor cortex to access bulbospinal pathways, such as the reticulospinal tract.

Such changes in brain networks can be indirectly detected by measuring spontaneous, low-frequency fluctuations in fMRI signals in the absence of a task. Correlations between signals in distinct brain regions when the subject is at rest, or resting-state functional connectivity (rsFC), can characterize motor networks, which would be active during movement (Biswal *et al.*, 1995). Because of the absence of an active task, this approach makes it possible to characterize motor networks in stroke individuals who may not be capable of performing a motor task.

Previous neuroimaging studies have described stroke-induced structural and functional changes in cortical regions, but give little attention to brainstem microstructure and functional organization. To date, it remains unknown whether rsFC to the brainstem is altered in chronic stroke. Therefore, we used a multi-modal neuroimaging approach to quantify structural and functional connectivity with the brainstem reticular formation in chronic stroke individuals compared with controls. Since patterns of rsFC can reflect functional organization of the brain, we predicted that individuals with stroke would show altered rsFC between contralesional cortex and brainstem regions that give rise to bulbospinal pathways, a pattern reflective of increased dependence upon these pathways after stroke-induced tissue damage. Studying brainstem motor networks in stroke can help us better understand their role in humans, in vivo, in both health and disease.

Here we identified significant rsFC and structural changes in chronic, hemiparetic stroke individuals (n=20) compared with healthy, age-matched controls (n=16). Importantly, contralesional gray matter density reflected the severity of motor impairment. These findings extend our previous report of altered white matter integrity in the bulbospinal pathways in stroke (Owen et al., 2017) by demonstrating that rsFC with the brainstem is altered in a pattern that supports increased dependence on contralesional corticobulbospinal pathways in chronic, hemiparetic stroke.

Methods

Participants

24 moderately to severely impaired stroke individuals (age=58.66$\pm$8.24 years), and 16 age-matched healthy controls (age=60.2$\pm$7.79 years) without known neurological abnormalities

were included in the study. Stroke subjects sustained a unilateral brain lesion at least four months prior to participation in the study.

Inclusion criteria for stroke individuals were as follows: 1) paresis confined to one side, with motor impairment of the upper limb, 2) participants with an overall Upper Extremity FMA score between 0 and 50 out of 66 (0-20=severe; 21-50=moderate (Velozo & Woodbury, 2011)), 3) absence of severe cognitive or affective dysfunction, 4) absence of severe concurrent medical problems. The protocol was approved by the Institutional Review Board at Northwestern University; all subjects provided a written informed consent.

Clinical Assessment

Upper extremity motor impairment was assessed in the paretic limb in stroke individuals using the Fugl-Meyer Assessment (FMA), a stroke-specific, performance-based motor impairment index, which measures loss of independent joint function, stretch reflex hyper-excitability and altered sensation (Fugl-Meyer *et al.*, 1975). It is one of the most widely used clinical scales of motor impairment post-stroke (Gladstone *et al.*, 2002). All assessments were performed by one licensed physical therapist to ensure consistency. Higher values indicated less impairment (range: 11 to 50 out of a maximum score of 66).

Data Acquisition

MRI scans were performed at Northwestern University's Center for Translation Imaging on a 3 Tesla Siemens Prisma scanner with a 64-channel head coil. Resting state functional data, based on the blood oxygenation level-dependent (BOLD) signal, were acquired (TR=679ms,

TE=22ms, flip angle=47º, 80 slices with slice thickness of 2mm, voxel size 2mm x 2mm x 2mm, covering the whole brain and brainstem, 1110 volumes collected), lasting 13 minutes. Participants were instructed to keep their eyes open, stay relaxed and let their minds wander during the scan.

Structural T1-weighted scans were acquired using an MPRAGE sequence (TR=2.3s, TE=2.94ms, field of view=256mm x 256mm) producing an isotropic voxel resolution of 1 mm x 1mm x 1mm and lasting 10 minutes.

Diffusion weighted images were collected from all subjects using spin-echo echo-planar imaging (TR=5s, TW=85ms, matrix size=150x150, FOV=225x225mm, slice thickness=1.5mm, interslice gap=0mm, number of slices=120) producing an isotropic voxel resolution of $1.5x1.5x1.5mm^3$ and lasting 5 minutes. The sequence consisted of diffusion weighting of $1000s/mm^2$ in 60 different directions and 8 scans with no diffusion weighting ($b=0s/mm^2$).

Functional data analysis

Preprocessing was carried out using Analysis of Functional NeuroImages (AFNI) software (afni.nimh.nih.gov). Data from 4 stroke participants were discarded from the resting state fMRI analyses due to excessive head movements (framewise displacement (FD) > 0.5). T1 images underwent brain extraction and segmentation into individual white matter, gray matter and CSF components. Brainstem regions were removed from the white matter mask, so that signals were not regressed out at later processing stages. Images were then non-linearly registered to a standard MNI 2mm brain template image.

Functional data underwent motion-based scrubbing/censoring with a framewise displacement threshold of .5 and DVARS value of 80, bandpass filtering between .01Hz and .1Hz and spatial smoothing using a Gaussian kernel of 4mm full width at half maximum. The T1 image was then aligned to the functional data, and mean CSF/white matter signals were extracted and regressed out. Boundary-Based Registration (Greve & Fischl, 2009) was used to align functional data to structural images. Structural images were then transformed to standard MNI space and the warp fields produced were applied to the functional statistical summary images.

A seed-based functional connectivity approach was used with defined seeds at the level of the caudal pons in the reticular formation in the left and right hemispheres. The averaged time-course of the voxels within each seed was tested for correlation with each of all other voxel time-courses of the brain. Pearson correlation coefficient maps were produced and then converted to z-values using Fisher's correction to improve normality. For stroke individuals with lesions in the left hemisphere, maps were flipped so that group analysis compared all contralesional hemispheres in the left hemisphere.

Statistical analysis was conducted using FMBIRB software library (FSL) (http://www.fmrib.ox.ac.uk/fsl). A voxel-wise general linear model (GLM) was implemented to test differences between the 3 groups (severely impaired, moderately impaired, control). Permutation testing was applied to the z-maps using 5,000 permutations with threshold-free cluster enhancement to correct for multiple comparisons. A threshold of $p<0.05$ was applied to the identified clusters.

Diffusion MRI data analysis

The diffusion-weighted images were first brain-extracted using the BET toolbox in FSL. The data were then denoised using an estimate of the noise variance in CSF signal intensity of the right ventricle (Aja-Fernandez *et al.*, 2008) and Rician noise corrected (Ingo *et al.*, 2014). The data were corrected for motion and eddy currents by co-registering diffusion weighted images to the image acquired with b=0s/mm^2 using the FLIRT toolbox in FSL. The motion correction transformation matrix was applied to the diffusion gradient directions to rotate them according to the registration algorithm. The pre-processed diffusion weighted data were fitted to a tensor on a voxel-wise basis using DTIFIT in the FSL Diffusion Toolbox (Behrens *et al.*, 2003).

For those individuals with lesions in the left hemisphere, FA maps were flipped so that all subjects had lesions in the right hemisphere and group analysis compared all contralesional hemispheres in the left hemisphere. FA maps were first linearly and then non-linearly registered to the FMRIB58_FA in Montreal Neurological Institute's (MNI) standard space. A mean FA image was then created from all individual FA images, and used to generate a common group skeleton. A threshold was applied at 0.2 to minimize potential white matter / gray matter partial volume effects. Finally, each FA image was projected onto the common group skeleton for subsequent statistical analysis in the brainstem white matter.

In order to determine voxel-wise statistics between severely impaired stroke, moderately impaired stroke and healthy control groups, permutation testing was applied to the 4D skeletonized FA in the brainstem. Using RANDOMISE in FSL, 5,000 permutations with

threshold-free cluster enhancement were performed to correct for multiple comparisons (Winkler *et al.*, 2014).

Voxel-based morphometry Analysis

Anatomical T1 scans were analyzed using FSL voxel-based-morphometry (VBM) (https://fsl.fmrib.ox.ac.uk/fsl/fslwiki/FSLVBM; Oxford University, Oxford, United Kingdom) (Ashburner & Friston, 2000; Whitwell, 2009) in FSL (Smith *et al.*, 2004). For those individuals with lesions in the left hemispheres, T1 images were flipped so that all subjects had lesions in the right hemisphere. The T1 images were then brain-extracted using the Brain Extraction Tool and segmented into gray matter (GM), white matter and cerebrospinal fluid using the FAST4 tool. The gray matter images were affine-registered to the gray matter ICBM-152 template, concatenated and then averaged to create a study-specific GM template. Individual GM images in native space were then non-linearly registered to this template using FNIRT. A voxel-wise General Linear Model was applied with Threshold-Free Cluster Enhancement (Winkler *et al.*, 2014) to detect changes in gray matter density between control, severely impaired and moderately impaired groups.

Results

Increased brainstem functional connectivity in stroke

Animal and human studies have demonstrated a direct, ipsilateral cortico-reticular projection from motor cortex to the reticular formation (Keizer & Kuypers, 1989; Jang & Seo, 2014, 2015; Fregosi *et al.*, 2017a), which could become increasingly important after stroke. We investigated functional connectivity between the origin of the reticulospinal tract in the brainstem

and contralesional motor cortex using a seed-based approach. Two seed-regions were defined in the left and right reticular formation (RF) in the pons, where part of the reticulospinal tract originates. Resting state functional connectivity was assessed between each seed region and contralesional cortex (dominant hemisphere in controls) in stroke individuals compared with controls.

Table 4.1

Significant clusters of voxels that showed higher functional connectivity with contralesional reticular formation in stroke when compared to controls.

Statistical Parametric Map	Voxels	X	Y	Z	Region
1	824	-20	-23	68.5	Left primary motor cortex/primary sensory cortex
2	288	-2	-21	-58	Left supplementary motor area/pre-supplementary area
3	43	-46	6	40	Left premotor area (ventral)
4	35	-42	2	54	Left premotor area (dorsal)
5	11	-54	10	36	Left premotor area (ventral)
6	7	58	68	61	Left premotor area (ventral)

Clusters of increased connectivity to the contralesional RF seed-region were identified in contralesional S1, M1, SMA, preSMA and PM cortical regions, listed in Table 4.1 and displayed on standard MNI brain in Figure 4.1. Increased connectivity to the ipsilesional RF seed-region was observed in a small cluster in contralesional PM cortex. For these results, there were no significant differences between moderately and severely impaired stroke groups. For both seed-regions, there were no voxels in which the control group had greater connectivity than the stroke group.
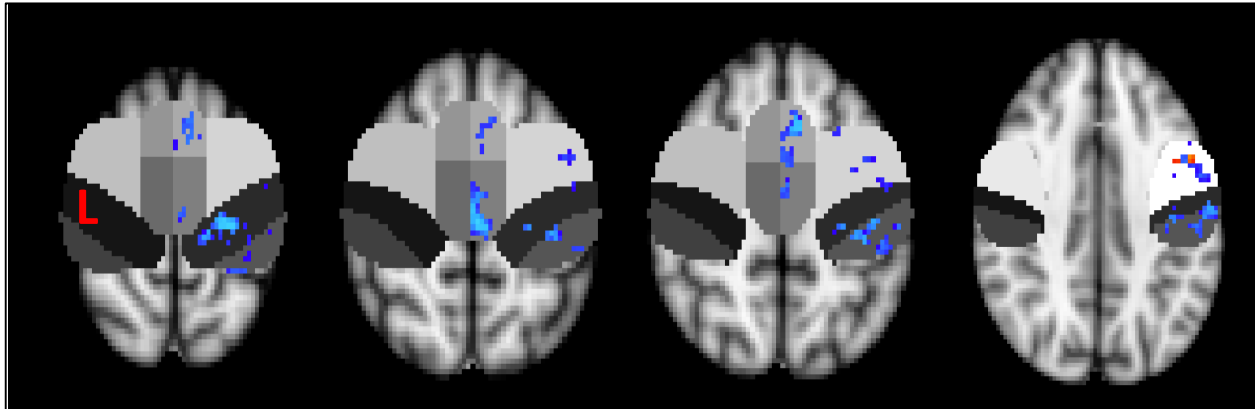
Figure 4.1
Resting state functional connectivity between contralesional reticular formation and contralesional sensorimotor cortex is increased in chronic stroke, shown in blue. Resting state functional connectivity between ipsilesional reticular formation and contralesional sensorimotor cortex is increased in chronic stroke, shown in red. L signifies lesioned hemisphere.

Altered white matter microstructure in stroke

The descending motor pathways, including the corticospinal tract, project from motor cortex and travel down through the ventral brainstem. Diffusion imaging can investigate microstructural tissue properties within these descending corticofugal pathways in the brainstem using fractional anisotropy (FA), a measurement thought to reflect myelination (Chang *et al.*, 2017a), but can also be sensitive to fiber density, fiber diameter, and membrane permeability (Jones *et al.*, 2013).

Both severely and moderately impaired stroke groups showed decreased FA in ipsilesional corticofugal pathways when compared to age-matched controls (p<0.0001), a pattern reflective of chronic white matter degeneration in the lesioned hemisphere. These results are displayed in Figure 4.2.
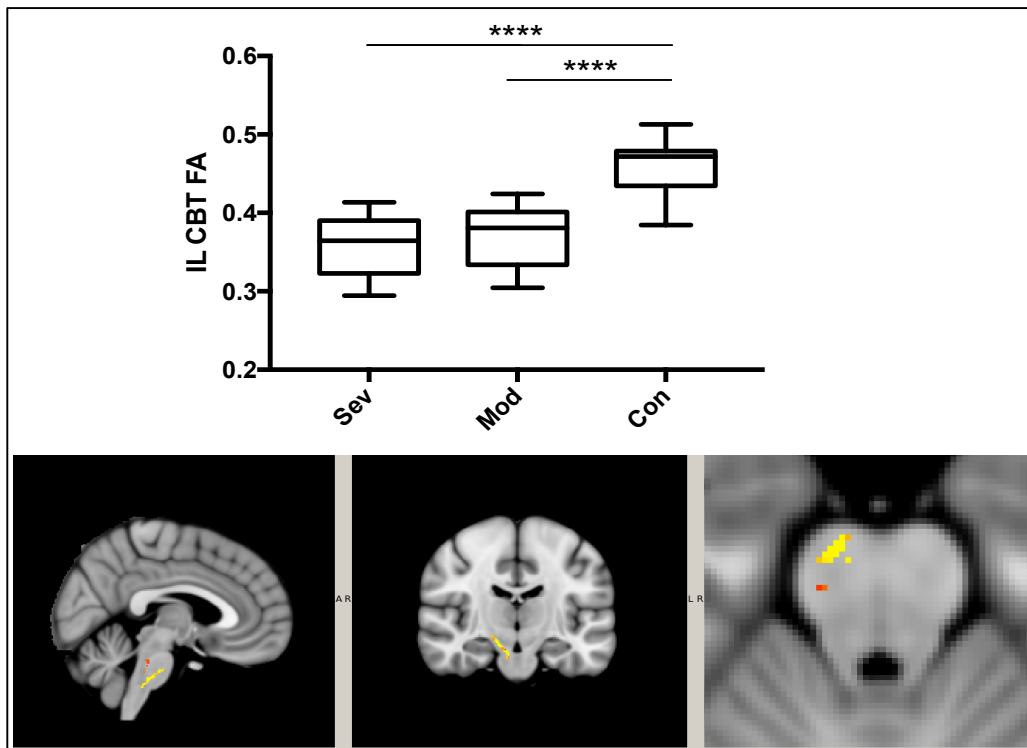
Figure 4.2
Both severely and moderately impaired stroke groups showed significantly decreased fractional anisotropy (FA) within ipsilesional corticofugal pathways when compared to healthy, age-matched controls (p<0.0001).

In contrast, severely impaired stroke individuals showed increased FA in contralesional corticofugal pathways when compared to moderately impaired (p=0.018) and control (p=0.0009) groups. There was no significant difference in FA between moderately impaired and control groups (p=0.69). These results are displayed in Figure 4.3. Together, these findings indicate that stroke participants with the most severe motor impairments in the upper extremity have decreased FA in ipsilesional corticofugal pathways and increased FA in contralesional

corticofugal pathways, a pattern reflective of reorganizational neural changes in brainstem white matter.
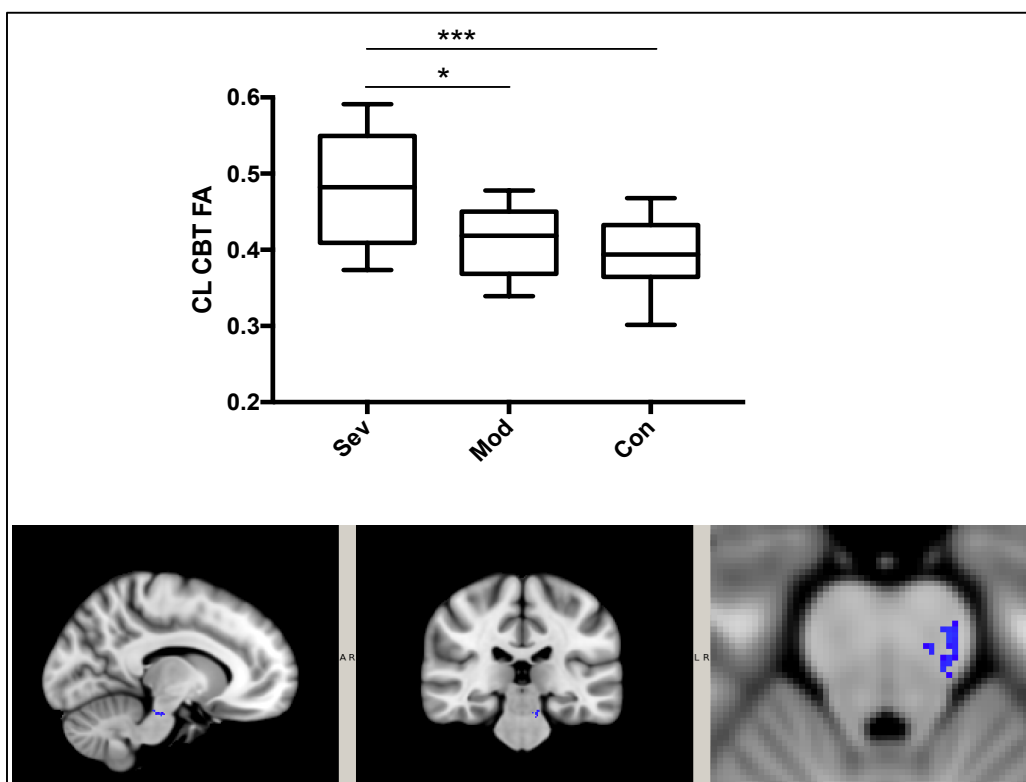
Figure 4.3
Severely impaired stroke individuals showed significantly increased fractional anisotropy (FA) within contralesional (CL) corticofugal pathways when compared to both moderately impaired stroke and control groups.

Altered gray matter density in stroke

Since we found altered brainstem resting state functional connectivity with the contralesional motor cortex in stroke compared to control, we tested whether there were any subsequent gray matter density changes that would reflect structural reorganization in stroke. We used a voxel-based morphometry approach to test whether there were group differences in gray matter density in the contralesional hemisphere.

Voxels on the boundary between primary motor cortex (M1) and premotor cortex (PM) showed significantly higher gray matter density in the most severely impaired stroke individuals when compared with the moderately impaired individuals (p=0.0023) and control groups (p=0.0272). There was no significant difference in gray matter density between moderately impaired and control groups (p=0.36). These results are displayed in Figure 4.4.

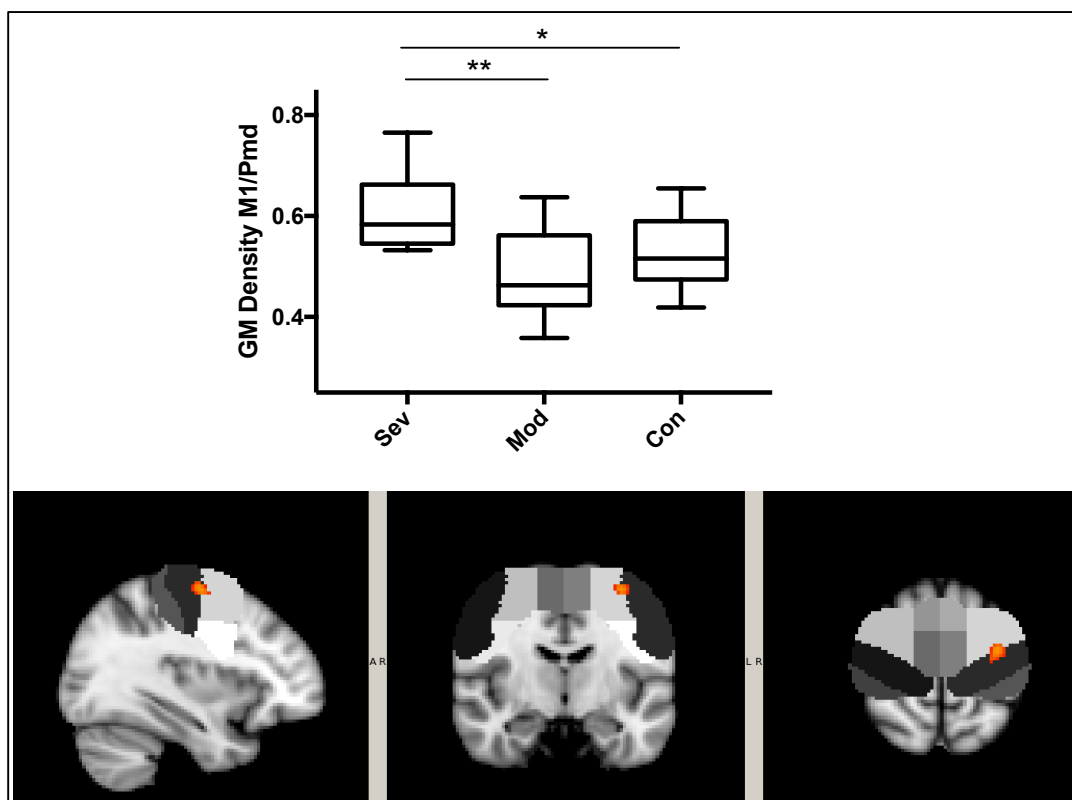**Figure 4.4**
Severely impaired stroke individuals showed significantly increased gray matter (GM) density in primary motor (M1) and premotor (PM) cortex when compared to moderately impaired stroke and control groups.

A correlation analysis performed between this cluster in M1/PM and the Fugl-Meyer assessment showed a significant negative correlation between gray matter density and

impairment severity (r=-0.58, p=0.0075). This result shows that stroke participants with the most severe impairment also demonstrate the highest gray matter density in M1/PM cortex.

Discussion

Summary of results

The purpose of this study was to evaluate whether resting state functional connectivity was altered in chronic, hemiparetic stroke when compared to healthy age-matched controls. Additionally, we sought to determine whether white and gray matter structural changes accompanied any functional changes. We found both functional and structural changes in stroke compared to controls, with the most pronounced differences present in severely impaired individuals.

Increased brainstem functional connectivity in stroke

For the first time, we show that resting state functional connectivity between contralesional motor cortex and brainstem structures is altered in chronic hemiparetic stroke. We found increased resting state functional connectivity between contralesional reticular formation and contralesional sensorimotor cortex (S1, M1, PM, SMA) in individuals with chronic stroke when compared to healthy age-matched control individuals.

It is clear that lesions can cause state changes in spontaneous functional architecture of the brain at rest. Although the exact relationship between rsFC and underlying neural activity is not fully understood, evidence suggests that resting-state networks reflect clusters of brain regions that coactivate during the performance of sensorimotor tasks (Fox & Raichle, 2007), and that the slow resting-state signal fluctuations are directly related to the same frequency range fluctuations

in the power of fast (gamma range) local field potentials (Leopold & Maier, 2012; Thiel & Vahdat, 2015).

Many previous studies have used rsFC to assess the health of brain networks in a wide range of disease states, with implications for prognosis and recovery. For example, in poorly recovered stroke patients, motor function correlated with the degree of decreased interhemispheric functional connectivity (Chen & Schlaug, 2013; Urbin *et al.*, 2014), and more specifically, patients with relatively poor hand function showed reduced interhemispheric M1-M1 connectivity (Carter *et al.,* 2010). Additionally, both intensive upper extremity rehabilitative training (Wittenberg *et al.*, 2016) and the use of interventional transcranial direct stimulation (tDCS) (Lefebvre *et al.*, 2017) have the ability to alter resting state networks. Without intervention, these networks seem to stabilize around 5 weeks post-stroke (Nijboer *et al.*, 2017).

Although many studies have shown altered rsFC in stroke, they have predominantly focused on cortico-cortical interactions and a few subcortical regions such as the thalamus and cerebellum (Park *et al.*, 2011). Despite work suggesting that bulbospinal pathways, such as the reticulospinal tract, could be important following stroke-induced tissue damage (Lawrence & Kuypers, 1968b, 1968a; Dewald *et al.*, 1995; Ellis *et al.*, 2012; Zaaimi *et al.*, 2012; Owen *et al.*, 2017), rsFC with the brainstem has not previously been investigated.

Animal and human studies have demonstrated a direct, ipsilateral cortico-reticular projection from motor cortex to the reticular formation (Keizer & Kuypers, 1989; Jang & Seo, 2014, 2015; Fregosi *et al.*, 2017a), providing a potential neuroanatomical pathway connecting contralesional motor cortex with brainstem regions and subsequently, through descending bulbospinal pathways, motor neurons in the spinal cord. Evidence from healthy controls suggests

that neuroplastic changes that occur during a motor learning paradigm display a highly reliable linear relationship with behavioral measures (Vahdat *et al.*, 2011), suggesting a direct link between rsFC and behavioral change. Based on this evidence, it is possible that the increased rsFC between contralesional motor cortex and reticular formation in stroke could reflect an increased reliance on contralesional cortico-reticular pathways to elicit movement in the paretic limb. While we have identified increased rsFC in chronic stroke individuals, more work is needed to further elucidate the time course of these changes from the acute phase to the chronic phase following stroke.

Altered white matter microstructure in stroke

In addition to altered rsFC in chronic stroke, we found significantly decreased FA in ipsilesional descending corticofugal tracts in both severely and moderately impaired individuals when compared to age-matched controls. This is consistent with white matter degeneration following neural injury (Concha *et al.*, 2006), and supports the findings of many other studies.

In contrast to this decrease in FA, we also observed an increase in FA in the contralesional corticofugal tracts in the severely impaired group when compared to moderately impaired and control groups. Diffusion imaging studies in healthy controls have shown that increased FA in white matter is associated with practice of a motor task (Scholz *et al.*, 2009), suggesting that increased use can increase FA. This evidence from healthy controls indicates that individuals with the most severe upper extremity impairment could be relying more heavily on contralesional corticofugal pathways to elicit movement of the paretic limb, albeit synergistic and dysfunctional in nature.

Altered gray matter density in stroke

We found that the severely impaired stroke group had significantly increased gray matter density in contralesional motor cortex (M1/PM cortex) when compared to moderately impaired and control groups. Gray matter plasticity has been associated with motor skill learning in healthy controls, showing increased gray matter density in days or weeks following training (Scholz *et al.*, 2009; Taubert *et al.*, 2010). These changes have been attributed to potential remodeling of dendritic spines and axonal terminals, glial hypertrophy, and synaptogenesis (Draganski & May, 2008; Dayan & Cohen, 2011). This evidence indicates that the increased gray matter density in M1/PM cortex could be a result of a more exclusive use of the contralesional M1/PM cortices in the most severely impaired group and subsequent neural plasticity detectable by MR approaches. Future work is needed to elucidate the time course of these changes and the exact underlying biology.

Contralesional structural changes in the most severely impaired individuals

Surprisingly, we did not find significant differences in contralesional white matter or gray matter density when comparing the moderately impaired stroke group with the control group. One possible explanation could be that the moderately impaired group shows a much less pronounced difference when compared to the control group that would require larger numbers to produce any significant difference. Alternatively, it could indicate something unique in the severely impaired individuals. In measuring motor impairment through more quantitative means using robotics, we have observed that individuals with the lowest FMA score, on average, are

able to lift around 1.5 times their limb weight before involuntary flexion drive prevents a voluntary reach forward. In contrast, the moderately impaired individuals are able to lift, on average, 2.5 times their limb weight before this occurs. Thus, it is possible that individuals with the most severe impairment could be using the contralesional cortico-reticular pathways for almost all movements, whereas the individuals with more moderate levels of impairment can perform many motor tasks without recruiting these contralesional pathways. More quantitative measurements of impairment are needed to further elucidate precisely how these altered neuroanatomic correlates contribute to loss of independent joint control post-stroke in future work.

Conclusion

Advances in modern neuroscience have shown that the plasticity of the brain extends beyond the previously accepted critical period during development. Plastic reorganization is conditional on the specific needs of the individual and can result in both beneficial or maladaptive consequences (Pascual-Leone *et al.*, 2005). Here we have demonstrated plastic reorganization in chronic hemiparetic stroke individuals, but future work will be necessary to address the specific timing of these structural and functional changes from the acute phase, as well as test whether interventions are possible to prevent these changes from developing.

5. Changes in Fractional Anisotropy and Functional Connectivity are Associated with a Loss of Independent Joint Control in Chronic Hemiparetic Stroke

Introduction

The leading hypothesis for a loss of independent joint control, resulting from the expression of the flexor synergy (i.e. abnormal coupling between shoulder abduction with elbow, wrist and finger flexion) in the paretic upper limb (Dewald & Beer, 2001) following stroke-induced damage to descending corticofugal pathways is an increased reliance on contralesional corticoreticulospinal motor pathways (Dewald *et al.*, 1995; McMorland *et al.*, 2015). There is indirect evidence to support this hypothesis in humans from work using TMS (Schwerin *et al.*, 2008; Schwerin *et al.*, 2011) and following manipulation of sensory input (McPherson *et al.*, 2008; Krainak *et al.*, 2011; Ellis *et al.*, 2012). However, direct neuroimaging evidence for changes in brain structure and function, explaining the prevalence of the flexion synergy in the paretic arm, has not yet been provided in humans post-stroke. Therefore, in the present study, we employ multi-modal structural and functional neuroimaging along with rehabilitation robotics (Ellis *et al.*, 2016) to evaluate the relationship between neural integrity/connectivity and the loss of independent joint control. Using this approach, we aimed to determine which neural substrates were sensitive to quantitative peripheral measurements of flexion synergy in the paretic upper limb as a function of shoulder abduction loading, and to test the hypothesis that an increased reliance on contralesional corticoreticulospinal pathways is related to loss of independent joint control in chronic stroke.

Evidence from animal and human studies suggests that the contralesional corticoreticulospinal pathway can contribute to flexion synergy after stroke. In a primate model, the reticulospinal tract makes mono- and di-synaptic connections with motor neurons controlling the forearm (Riddle *et al.*, 2009), and stimulation of the reticular formation produces wrist flexor/elbow flexor/shoulder abductor activation in the ipsilateral limb (Davidson & Buford, 2006), mirroring the flexion synergy pattern observed in humans after stroke. Anterograde tracing shows a direct, ipsilateral projection from motor cortex to the reticular formation in macaques, predominantly from premotor and supplementary cortical regions (Fregosi *et al.*, 2017b), and diffusion tractography can detect this pathway in humans (Jang & Seo, 2014). Furthermore, following stroke-induced damage, the contralesional reticulospinal tract can strengthen its connections to forearm muscles in primates (Zaaimi *et al.*, 2012) and become upregulated in humans (Schwerin *et al.*, 2008; Schwerin *et al.*, 2011; Ellis *et al.*, 2012), demonstrating its ability for compensatory plastic changes after neural injury. Although individuals may be able to rely on alternative pathways after stroke-induced neural damage, motor function may be limited to synergistic and dysfunctional movement patterns.

Such reorganizational structural changes can be measured: gray matter density from a T1 scan and white matter microstructure from a diffusion weighted scan. Functional changes can be indirectly detected by measuring spontaneous, low-frequency fluctuations in fMRI signals in the absence of a task. Correlations between signals in distinct brain regions when the subject is at rest, or resting-state functional connectivity (rsFC), can characterize motor networks, which would be active during movement (Biswal *et al.*, 1995).

The impact of synergies on movement function is most commonly measured using the Fugl-Meyer Assessment (Fugl-Meyer *et al.*, 1975) through observational analysis on an ordinal scale. The assessment scale is composed of movement tasks "within synergy," "mixing synergy," and "out of synergy" producing a generalized motor impairment score out of 66 points. However, flexion synergy impairment is progressively expressed as a function of drive to the shoulder abductors during shoulder/elbow tasks whether in a static (Beer *et al.*, 1999; Dewald & Beer, 2001; Ellis *et al.*, 2007) or dynamic (Beer *et al.*, 2004; Sukal *et al.*, 2007; Ellis *et al.*, 2008) environment. Therefore, in order to quantify the magnitude or severity of flexion synergy, one must directly measure its impact on reaching function. This can be accomplished using a robotic device capable of quantifying the precise shoulder abduction loading threshold at which flexion synergy arrests reaching function. Concurrent evaluation of neural structure and functional connectivity along with the expression of flexion synergy affords the opportunity to establish a direct link between the neural mechanism and the motor impairment. Evidence is provided suggesting a direct and significant relationship between changes in neural structure and function with the expression of flexion synergy. A better understanding of the neural mechanisms associated with loss of independent joint control in stroke informs clinical practice and will facilitate the development of more targeted interventions for stroke rehabilitation.

Materials and methods

Participants

24 moderately to severely impaired stroke individuals (age=58.66$\pm$8.24 years), and 16 age-matched healthy controls (age=60.2$\pm$7.79 years) without known neurological abnormalities

were included in the study. Stroke subjects sustained a unilateral brain lesion at least four months prior to participation in the study.

Inclusion criteria for individuals with stroke were as follows: 1) paresis confined to one side, with motor impairment of the upper limb, 2) participants with an overall Upper Extremity FMA score between 12 and 45 out of 66, 3) ability to follow a three step command 4) absence of severe concurrent medical problems (self-report). The protocol was approved by the Institutional Review Board at Northwestern University; all subjects provided a written informed consent.

Imaging data acquisition

MRI scans were performed at Northwestern University's Center for Translation Imaging on a 3 Tesla Siemens Prisma scanner with a 64-channel head coil. Structural T1-weighted scans were acquired using an MPRAGE sequence (TR=2.3s, TE=2.94ms, field of view=256mm x 256mm) producing an isotropic voxel resolution of 1 mm x 1mm x 1mm and lasting 10 minutes. Diffusion weighted images were collected from all subjects using spin-echo echo-planar imaging (TR=5s, TW=85ms, matrix size=150x150, FOV=225x225mm, slice thickness=1.5mm, interslice gap=0mm, number of slices=120) producing an isotropic voxel resolution of $1.5x1.5x1.5mm^3$ and lasting 5 minutes. The sequence consisted of diffusion weighting of $1000s/mm^2$ in 60 different directions and 8 scans with no diffusion weighting ($b=0s/mm^2$).

Resting state functional data, based on the blood oxygenation level-dependent (BOLD) signal, were acquired (TR=679ms, TE=22ms, flip angle=47°, 80 slices with slice thickness of 2mm, voxel size 2mm x 2mm x 2mm, covering the whole brain and brainstem, 1110 volumes

collected), lasting 13 minutes. Participants were instructed to keep their eyes open, stay relaxed and let their minds wander during the scan.

Diffusion MRI data analysis

The diffusion-weighted images were first brain-extracted using the BET toolbox in FSL. The data were then denoised using an estimate of the noise variance in CSF signal intensity of the right ventricle (Aja-Fernandez *et al.*, 2008) and Rician noise corrected (Ingo *et al.*, 2014). The data were corrected for motion and eddy currents by co-registering diffusion weighted images to the image acquired with b=0s/mm^2 using the FLIRT toolbox in FSL. The motion correction transformation matrix was applied to the diffusion gradient directions to rotate them according to the registration algorithm. The pre-processed diffusion weighted data were fitted to a tensor on a voxel-wise basis using DTIFIT in the FSL Diffusion Toolbox (Behrens *et al.*, 2003).

For those individuals with lesions in the left hemisphere, FA maps were flipped so that all subjects had lesions in the right hemisphere and group analysis compared all contralesional hemispheres in the left hemisphere. FA maps were first linearly and then non-linearly registered to the FMRIB58_FA in Montreal Neurological Institute's (MNI) standard space. A mean FA image was then created from all individual FA images, and used to generate a common group skeleton. A threshold was applied at 0.2 to minimize potential white matter / gray matter partial volume effects. Finally, each FA image was projected onto the common group skeleton for subsequent statistical analysis in the brainstem white matter.

A voxel-wise general linear model (GLM) was implemented determine if any voxels were sensitive to impairment severity. Using RANDOMISE in FSL, 5,000 permutations with threshold-free cluster enhancement were performed (Winkler *et al.*, 2014). A threshold of $p<0.05$ was considered significant.

Voxel-based morphometry analysis

Anatomical T1 scans were analyzed using FSL voxel-based-morphometry (VBM) (https://fsl.fmrib.ox.ac.uk/fsl/fslwiki/FSLVBM; Oxford University, Oxford, United Kingdom) (Ashburner & Friston, 2000; Whitwell, 2009) in FSL (Smith *et al.*, 2004). For those individuals with lesions in the left hemispheres, T1 images were flipped so that all subjects had lesions in the right hemisphere. The T1 images were then brain-extracted using the Brain Extraction Tool and segmented into gray matter (GM), white matter and cerebrospinal fluid using the FAST4 tool. The gray matter images were affine-registered to the gray matter ICBM-152 template, concatenated and then averaged to create a study-specific GM template. Individual GM images in native space were then non-linearly registered to this template using FNIRT. A voxel-wise General Linear Model was applied with Threshold-Free Cluster Enhancement (Winkler *et al.*, 2014) to determine if any voxels were sensitive to impairment severity. A threshold of $p<0.01$ was considered significant.

Functional data analysis

Preprocessing was carried out using customized Northwestern pipelines (Song, 2015). Data from 4 stroke participants were discarded from the resting state fMRI analyses due to

excessive head movements (framewise displacement (FD) > 0.5). T1 images underwent brain extraction and segmentation into individual white matter, gray matter and CSF components. Brainstem regions were removed from the white matter mask, so that signals were not regressed out at later processing stages. Images were then non-linearly registered to a standard MNI 2mm brain template image.

Functional data underwent motion-based scrubbing/censoring with a framewise displacement threshold of .5 and DVARS value of 80, bandpass filtering between .01Hz and .1Hz and spatial smoothing using a Gaussian kernel of 4mm full width at half maximum. The T1 image was then aligned to the functional data, and mean CSF/white matter signals were extracted and regressed out. Boundary-Based Registration (Greve & Fischl, 2009) was used to align functional data to structural images. Structural images were then transformed to standard MNI space and the warp fields produced were applied to the functional statistical summary images.

A seed-based functional connectivity approach was used with defined seeds at the level of the caudal pons in the reticular formation in the left and right hemispheres. The averaged time-course of the voxels within each seed was tested for correlation with each of all other voxel time-courses of the brain. Pearson correlation coefficient maps were produced and then converted to z-values using Fisher's correction to improve normality. For stroke individuals with lesions in the left hemisphere, maps were flipped so that group analysis compared all contralesional hemispheres in the left hemisphere.

Statistical analysis was conducted using FMRIB software library (FSL) (http://www.fmrib.ox.ac.uk/fsl). A voxel-wise general linear model (GLM) was implemented

determine if any voxels were sensitive to impairment severity. Permutation testing was applied to the z-maps using 5,000 permutations with threshold-free cluster enhancement. A threshold of p<0.01 was considered significant.

Figure 5.1
Robotic set up in the ACT[3D]. Subjects are seated and given visual feedback.

Quantification of synergy expression using robotics

The robotic protocol consisted of two main components. A more detailed version of the protocol was previously described (Ellis *et al.*, 2016). First, the participant's maximum shoulder abduction force was obtained to normalize abduction loading across participants and minimize effects of strength/weakness, which could confound results. The participant was seated and strapped in a Biodex3 chair with their arm resting in a forearm-hand orthosis attached to the ACT[3D], shown in Figure 5.1. The participant's arm was placed into a "home position", which aligned the shoulder 90º to the line of gravity and the upper arm 40º anterior to the anatomical frontal plane, with the elbow angle placed at 70º. This standardized home position was used to generate a graphic representation of the arm displayed on a screen in front of the participant. Multiple repetitions of maximum shoulder abduction were completed until 3 values that were within 10% of one another were obtained (Dewald & Beer, 2001).

Second, the subject's maximum reaching abduction load (MRAL$_{near}$) was determined (see Ellis et al 2016). The MRAL$_{near}$ measures the magnitude of loss of independent joint control or flexion synergy impairment. It determines the synergy take-over threshold where the participant

is no longer able to overcome flexion synergy and initiate a reaching motion. A binary decision tree algorithm is implemented to rapidly identify the maximum abduction load at which the participant can no longer successfully initiate reaching. With their arm supported on the haptic table, participants are instructed to start with their arm just behind the close target (hand approximated with the torso). Participants were instructed to first lift the arm up and then attempt to initiate reaching toward the close target. Subjects were given up to 3 attempts to successfully complete the task. If they were successful, the next load was increased by 50% of the remaining load range, if not, the next load was decreased by 50%. The $MRAL_{near}$ value can be determined in 5 steps achieving a measurement resolution to the nearest 3.125%. In the results section $MRAL_{near}$ is referred to as "independent joint control" for greater clarity. A lower value signifies greater loss of independent joint control, whereas a higher value signifies better performance on the robotic task.

Results

White matter sensitive to synergy severity

A voxel-wise GLM analysis on FA maps was carried out to determine whether any brainstem voxels were sensitive to a quantitative measurement of independent joint control. We found significant voxels both positively and negatively related to independent joint control in stroke. A positive correlation was found in voxels primarily clustered in ipsilesional cerebral peduncle, shown in Figure 5.2. Average FA values within these significant clusters were extracted and plotted against independent joint control. Individuals with the greatest losses of independent joint control showed the lowest FA values in voxels predominantly clustered in ipsilesional corticofugal pathways.
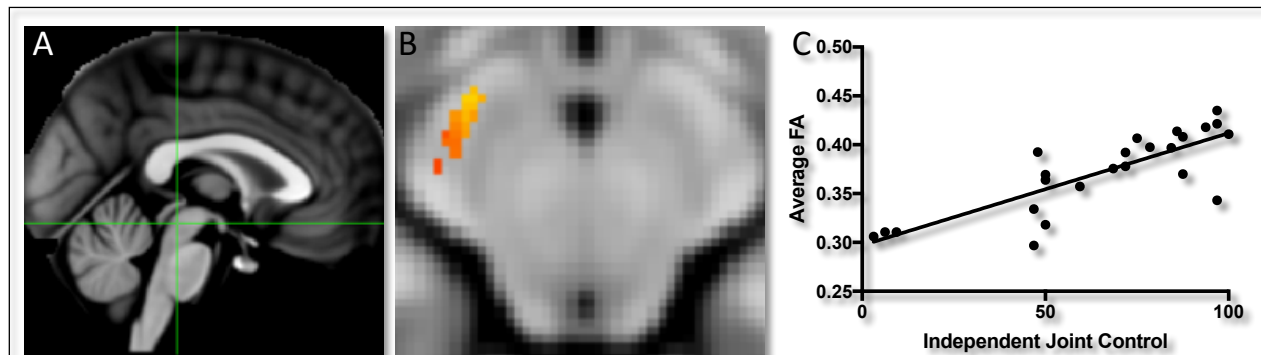
Figure 5.3
White matter voxels that significantly correlate positively with independent joint control. (A) Sagittal section of MNI standard brain showing the brainstem level of slice shown in (B). Horizontal section showing the midbrain cerebral peduncle with voxels positively correlated with independent joint control shown in red-yellow (spectrum signifying p-value: red=0.05; yellow=0). (C) Average FA values extracted from GLM results and plotted against loss of independent joint control (r=0.8, p<0.0001).

A negative correlation was found in voxels primarily in contralesional ventral pontine region where corticofugal tracts descend, shown in Figure 5.3. Average FA values within these significant clusters were extracted and plotted against independent joint control. Individuals with the greatest losses of independent joint control showed the highest FA in voxels predominantly

Figure 5.2
White matter voxels that significantly correlate negatively with independent joint control. (A) Sagittal section of MNI brain showing the brainstem level of slice shown in (B). Horizontal section showing the ventral pons with voxels negatively correlated with independent joint control shown in dark blue-light blue (spectrum signifying p-value: dark blue=0.05; light blue=0). (C) Average FA values extracted from GLM results and plotted against loss of independent joint control (r=-0.68, p=0.0003).

clustered in contralesional corticofugal tracts.

We hypothesized that FA in the ipsilesional cerebral peduncle would relate to FA in the contralesional cerebral peduncle. There was a weak but significant correlation between the two (r=-0.42, p=0.037).

Gray matter sensitive to synergy severity

A voxel-wise GLM analysis using the gray matter density maps was carried out to determine whether any voxels in the contralesional sensorimotor cortex gray matter were sensitive to a quantitative measurement of independent joint control. We observed a cluster in contralesional premotor cortex that showed a negative correlation with independent joint control. Individuals with the greatest losses in independent joint control, or the strongest expression of flexion synergy at the elbow during shoulder abduction, had the highest gray matter density
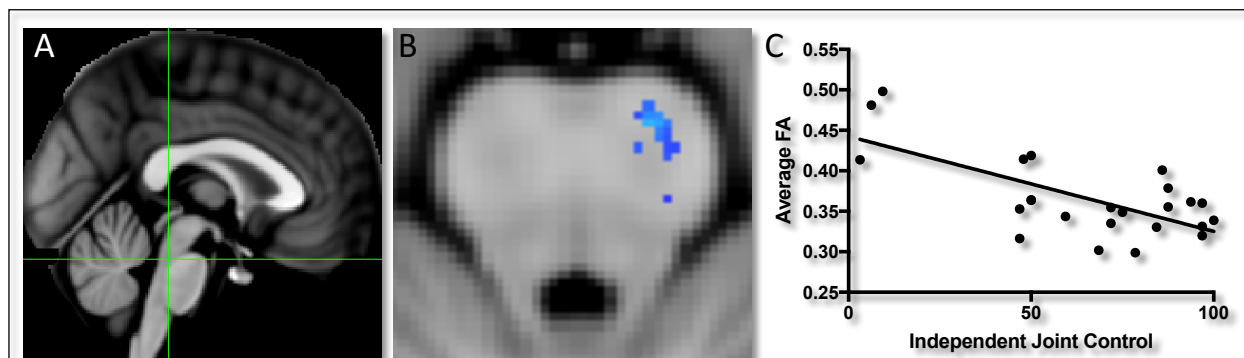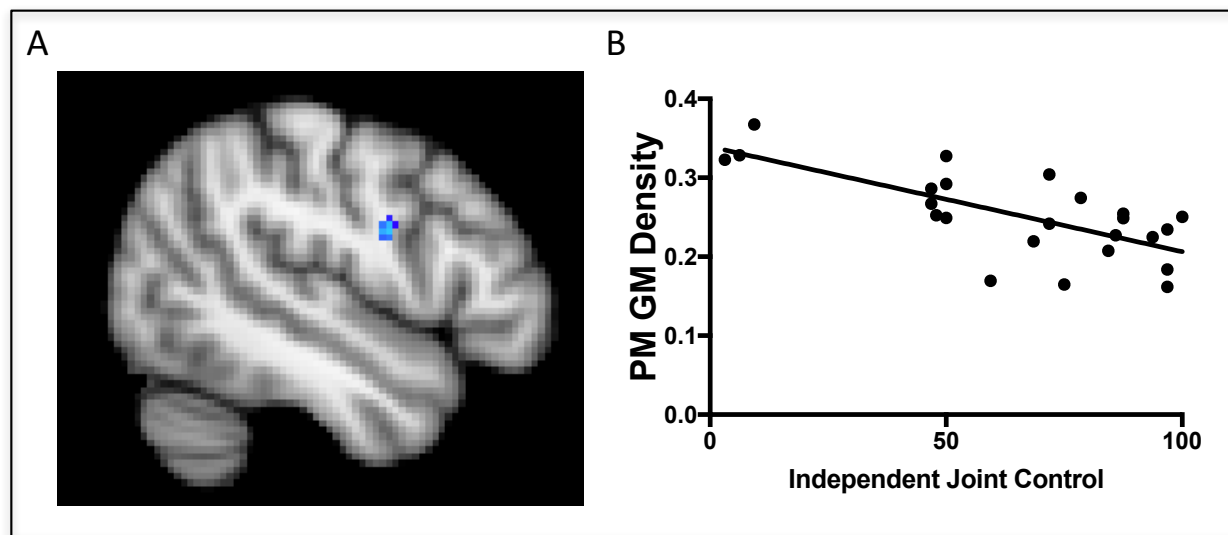

Figure 5.4
Gray matter voxels that significantly correlate negatively with independent joint control. (A) Sagittal section of MNI standard brain showing the significant cluster in contralesional premotor cortex, shown in blue. (B) Average FA values were extracted from GLM results and plotted against loss of independent joint control (p=-0.707, p=0.0001).

values in a cluster of voxels in contralesional premotor cortex. Average gray matter density values were extracted and plotted against independent joint control in Figure 5.4. No voxels showed a significant positive correlation with independent joint control in the contralesional sensorimotor cortex.

rsFC between contralesional RF and PM cortex sensitive to synergy severity

A voxel-wise GLM analysis using the resting state functional connectivity map between contralesional reticular formation in the brainstem and contralesional motor cortex was carried out to test whether any voxels' rsFC values were sensitive to loss of independent joint control. We observed a cluster in contralesional premotor cortex that showed a negative correlation with independent joint control. In other words, individuals who had greater rsFC between contralesional reticular formation and premotor cortex had more severe expression of flexion
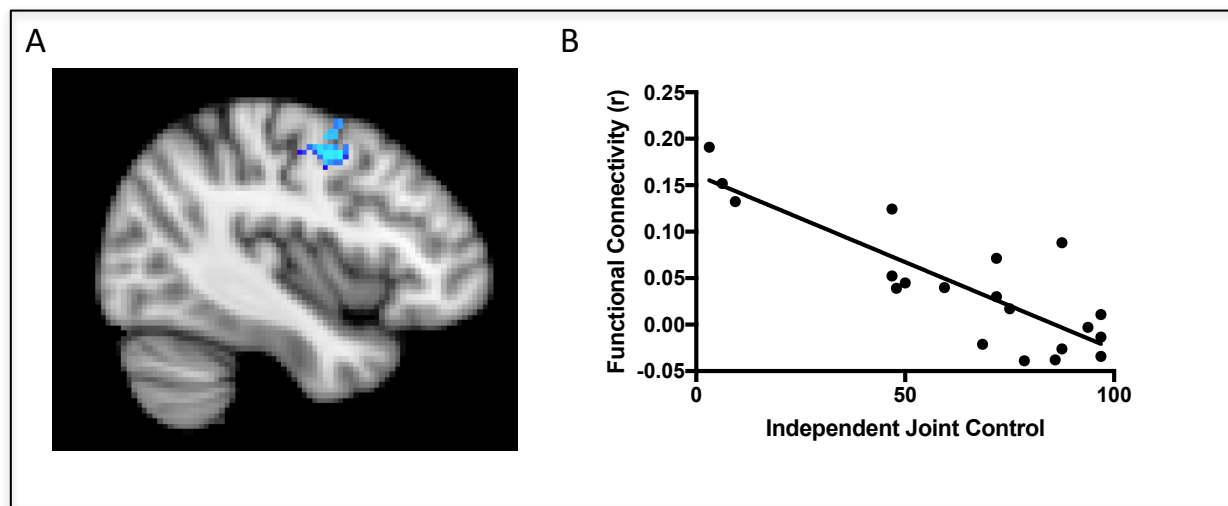
Figure 5.5
Voxels in contralesional sensorimotor whose functional connectivity with contralesional reticular formation significantly correlate negatively with independent joint control. (A) Sagittal section of MNI standard brain showing the significant cluster in contralesional premotor cortex, shown in blue. (B) Average rsFC r values were extracted from GLM results and plotted against loss of independent joint control (p=-0.84, p<0.0001).

synergy, or greater loss of independent joint control. Average rsFC r-values in the premotor cluster were extracted and plotted against independent joint control in Figure 5.5. No voxels in the FC map between contralesional reticular formation and contralesional sensorimotor cortex showed a significant positive correlation with independent joint control.

Gray matter correlates with rsFC

We found that resting state functional connectivity between contralesional reticular formation and contralesional premotor cortex and gray matter density in contralesional premotor cortex were both negatively correlated with independent joint control in chronic stroke individuals. Therefore, we tested to see whether the resting state functional connectivity average

Figure 5.6
Resting state functional connectivity between contralesional reticular formation and contralesional premotor cortex significantly correlates with gray matter (GM) density contralesional premotor (PM) cortex (r=0.612, p=0.0041).

r-value in premotor cortex was correlated with the gray matter density average in premotor cortex. We found a significant, positive correlation between the two values (r=0.612, p=0.0041), shown in Figure 5.6.
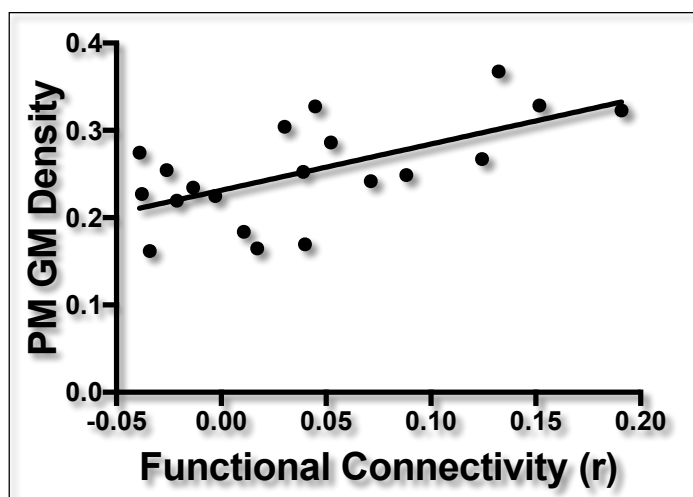
Discussion

Summary of results

In this study, we aimed to determine which, if any, neural substrates were specifically sensitive to a quantitative peripheral measurement of the flexion synergy, at the paretic arm as a function of shoulder abduction loading, and to test the hypothesis that an increased reliance on contralesional corticoreticulospinal pathways is related to loss of independent joint control in chronic stroke individuals. We predicted that if this were the case, we would see both structural and functional neuroanatomical correlates. We found specific relationships between independent joint control and white matter, gray matter and contralesional resting state cortical-brainstem functional connectivity that support our hypothesis.

Degeneration of ipsilesional pathways post-stroke

Previously we showed that in both moderately and severely impaired chronic stroke individuals, FA in ipsilesional white matter is decreased compared to healthy age-matched controls (Figure 4.2); however, we did not see a significant difference between the two stroke groups separated based on FMA alone. In the present study, we found a close correlation between a specific subset of voxels within the ipsilesional cerebral peduncle, which contain descending corticospinal and corticobulbar pathways, and loss of independent joint control (Figure 5.1). Individuals with greater loss of independent joint control showed the lowest FA

values in this region, indicative of the greatest losses in ipsilesional motor pathways. Such a

drop in FA is consistent with white matter degeneration following neural injury (Concha *et al.*, 2006). This finding indicates that more quantitative metrics of upper limb motor impairment are needed to allow for the determination of relationships between motor impairment measurements and changes in anatomical substrates obtained from structural MR neuroimaging techniques.

Plasticity within contralesional pathways post-stroke

Previously we showed that the most severely impaired stroke individuals exhibit increased FA in contralesional corticofugal pathways when compared to both moderately impaired individuals and healthy age-matched controls (Figure 4.3). In the present study, we expand upon this finding by demonstrating a correlation between a quantitative measurement of independent joint control and FA in these contralesional corticofugal pathways. Individuals with the greatest losses in independent joint control showed the highest FA values in these pathways.

Diffusion imaging studies in healthy controls demonstrate that practice of a motor task can increase FA within related white matter pathways (Scholz *et al.*, 2009), showing that increased use can increase FA. Therefore, our finding that individuals with the most severe expressions of flexion synergy also have the highest FA values in contralesional corticofugal pathways could indicate neuroplastic reorganization indicative of increased use in order to elicit movement in the paretic limb, albeit dysfunctional in nature.

Surprisingly, the ipsilesional and contralesional corticofugal FA values only loosely correlated, aligning with previous work suggesting synergistic but independent contributions from corticofugal sub-components to motor impairment post-stroke (Schulz *et al.*, 2017).

Gray matter sensitive to synergy severity

Previously we showed that the most severely impaired stroke individuals exhibit increased gray matter density in contralesional motor cortex when compared to both moderately impaired individuals and healthy age-matched controls (Figure 4.4). In the present study, we found a correlation between gray matter density in the contralesional hemisphere and loss of independent joint control. Individuals with the most severe expression of flexion synergy exhibited the highest gray matter density in contralesional premotor cortex.

This finding supports previous work that shows contralesional premotor cortex can contribute to movement after stroke, particularly in the most severely impaired individuals. Disrupting contralesional premotor activity using TMS slows finger movements in stroke participants when compared with controls (Johansen-Berg *et al.*, 2002), showing that premotor cortical activity actively contributes to movement production in severely impaired individuals. Additionally, MEPs produced by TMS of the ipsilateral (contralesional) cortex are most common in moderately to severely impaired individuals, and the delayed timing of the response, compared to the corticospinal tract, suggests an oligosynaptic corticobulbospinal pathway (Schwerin *et al.*, 2008). We build on these findings by showing that contralesional premotor cortex, in particular, is sensitive to loss of independent joint control in chronic stroke.

rsFC between contralesional RF and PM cortex is sensitive to synergy severity

Previously we showed that in stroke, when compared to healthy age-matched controls, resting state functional connectivity between contralesional reticular formation and contralesional motor cortex is increased (Figure 4.1). In this study, we expand upon those

findings by demonstrating that resting state functional connectivity between contralesional reticular formation and contralesional premotor cortex, in particular, is sensitive to independent joint control. Those individuals with the greatest expression of flexion synergy have the highest functional connectivity between these two regions.

Although the exact relationship between rsFC and underlying neural activity is not fully understood, evidence suggests that resting-state networks reflect clusters of brain regions that coactivate during the performance of sensorimotor tasks (Fox & Raichle, 2007). Based on this evidence, it is possible that the increased functional connectivity between contralesional reticular formation and contralesional premotor cortex could reflect increased use during movement. For those individuals that can barely lift their limb weight before the synergy expression overrides their voluntary drive to reach outwards, these pathways could become activated much more easily.

Although many studies have shown altered rsFC in stroke, they have predominantly focused on cortico-cortical interactions and a few subcortical regions such as the thalamus and cerebellum (Park *et al.*, 2011). Despite work suggesting that bulbospinal pathways, such as the reticulospinal tract, could be important following stroke-induced tissue damage (Lawrence & Kuypers, 1968b, 1968a; Dewald *et al.*, 1995; Ellis *et al.*, 2012; Zaaimi *et al.*, 2012; Owen *et al.*, 2017), rsFC with the brainstem has not previously been investigated.

Animal and human studies have demonstrated a direct, ipsilateral cortico-reticular projection from motor cortex to the reticular formation (Keizer & Kuypers, 1989; Jang & Seo, 2014, 2015; Fregosi *et al.*, 2017a), providing a potential neuroanatomical pathway connecting contralesional motor cortex with brainstem regions. Anterograde tracing demonstrated a dense,

ipsilateral corticobulbar projection from premotor cortex to several nuclei of the brainstem reticular formation, the origins of the reticulospinal tract. This corticobulbar projection originating in premotor cortex was more dense than the projection originating from primary motor cortex (Fregosi *et al.*, 2017b). In this study, we demonstrate for the first time, that there is a direct link between flexion synergy severity and increased rsFC between the origin of the reticulospinal tract and contralesional premotor cortex, suggesting that this connection is present in humans and could become upregulated post-stroke.

Limitations

The present study uses MR imaging techniques to assess neural mechanism behind abnormal joint torque coupling in chronic stroke individuals. We show correlations between neural structure, functional connectivity and a quantitative measurement of flexion synergy in stroke. However, we cannot definitively answer the question of causation because we cannot directly measure brain activity during movement with these MR techniques (mainly for reasons relating to motion artifacts caused by movement in the scanner). Previous studies have used techniques, such as EEG, to measure cortical activity during movements of the paretic limb, but this approach cannot measure brainstem structure or function. We interpret our results as an indication of long-term increased use of contralesional corticoreticulospinal pathways in the most severely impaired individuals, but future work should combine these various imaging modalities to further explain causation of loss of independent joint control post-stroke.

Conclusion

We present measurements of white matter, gray matter, and functional connectivity that are associated with a loss of independent joint control in chronic stroke. By using a multi-modal imaging approach combined with quantitative measurements of flexion synergy, we were able to identify specific anatomical regions associated with this impairment. A better understanding of the neural mechanisms underlying abnormal flexion synergies post-stroke will help develop more effective science-based rehabilitative interventions, aimed specifically at decreasing abnormal coupling of the joints in the paretic limb.

6. **Conclusion**

There are as many as 1.1 million hemiparetic stroke survivors in the United States who exhibit movement impairments. One fundamental example is the loss of independent joint control that results from an involuntary synergic coupling between shoulder abduction and elbow, wrist and finger flexion. It can also be described as a dynamic and task-dependent reduction of joint-individuation related to proximal joint utilization. It still remains unclear which specific neuroanatomical substrates and processes underlie the development of this debilitating motor impairment.

This work tested the hypothesis that following stroke-induced damage to ipsilesional descending motor pathways, contralesional cortibobulbospinal pathways, such as the corticoreticulospinal tract, become upregulated. There is indirect evidence to support this hypothesis from previous work done in humans and animals, but a direct evaluation of neural structure and function in the human brainstem in chronic stroke had not been carried out.

The work presented in this dissertation examines the role that the brainstem plays in loss of independent joint control in chronic hemiparetic stroke. Neuroanatomical substrates of motor deficits following stroke have predominantly been studied in cortical regions and focused on white matter integrity within the descending corticospinal tract. While much work has been done to document how ipsilesional corticospinal tract integrity and volume are important components in determining overall recovery potential, this alone cannot fully explain the specific emergence of involuntary abnormal joint coupling after stroke.

This work is the first concurrent evaluation of the neuroimaging substrates in the brainstem and a metric of independent joint control in chronic stroke. More specifically, a multi-modal

neuroimaging approach combined with quantitative robotics is used to explore the role the brainstem plays in the emergence of involuntary joint coupling in stroke.

Comparison of white matter microstructural properties between stroke and control groups shows decreased integrity in ipsilesional cerebral peduncle, bilateral corona radiata and the body of the corpus callosum in stroke, suggesting widespread degenerative changes even in areas distant from the lesion. In contrast, white matter integrity in the contralesional reticulospinal tract is the highest in those individuals with the most severe impairments compared to those with moderate impairments and controls. Microstructural integrity within the contralesional reticulospinal tract correlates significantly with both upper extremity synergy severity and hand impairment. Additionally, microstructural integrity in the ipsilesional rubrospinal tract significantly correlated with hand impairment severity. These findings show that individuals with the most severe motor impairments in the upper extremity after stroke have the highest white matter integrity in bulbospinal pathways and suggest that these pathways are being used more to elicit movement in the paretic limb.

In addition to these white matter structural differences, stroke subjects display increased resting state functional connectivity between contralesional brainstem and sensorimotor cortex when compared to the control subjects. Specifically, the functional connectivity between contralesional reticular formation and contralesional premotor cortex is significantly correlated with loss of independent joint control in stroke: those individuals with greater losses show higher functional connectivity. This finding reflects what was observed in white matter microstructure in the contralesional reticulospinal tract, suggesting that individuals with the most severe loss of independent joint control are relying more on contralesional corticoreticulospinal pathways.

The quantitative robotic metric shows that individuals that were classified in the severely impaired group had involuntary flexor drive override voluntary extension at 1.5 times limb weight, on average. In contrast, individuals classified in the moderately impaired group could lift an average of 2.5 times their limb weight before their voluntary drive was outweighed by the involuntary synergistic drive. This evidence suggests that the most severely impaired stroke group can perform few, if any, movements that don't activate the contralesional corticoreticulospinal pathways, which contribute to the involuntary flexion synergy, whereas the moderate group may activate them much less frequently, able to use other ipsilesional pathways in conjunction. This difference in recruitment could be what is reflected in the anatomical white matter and gray matter patterns observed in Chapter 4.

By combining neuroimaging to quantify changes in the brain with engineering approaches to study motor behavior, this dissertation demonstrates specific structural and functional changes in the corticoreticulospinal system. Future work will further elucidate the role of the rubrospinal pathway and distinguish between magno and parvocellular subdivisions of the red nucleus. Diffusion imaging evidence shows that white matter in the rubrospinal pathway was highest in individuals with the most severe hand impairment. Preliminary evidence from resting state functional connectivity analysis also suggests that functional connectivity with the red nucleus is altered in stroke. Future work will further describe these changes and separate the specific contributions each brainstem area and pathway can make towards movement after stroke.

Additionally, the present body of work analyzed 24 individuals in the chronic stage of stroke. Many of the subjects were years or even decades out from their stroke. It will be important for future work to characterize how these shifts occur over time from the acute phase

into the chronic, and to determine whether any interventions might alter the progression. It is possible that early therapeutic or stimulation interventions could change the progression. Given that the human brain remains plastic throughout life to varying degrees, it is also possible, as shown in earlier work (Ellis *et al.*, 2009a; Ellis *et al.*, 2009b) that interventions, even in the chronic phase, do have some effect.

In individuals with the most severe impairments the brain is not able to depend on normal pathways and the subsequent use of these "backup pathways" is the best output possible. Previous work has demonstrated that shifting cortical activity back to the ipsilesional motor cortex results in improved motor control of the hand (Wilkins, 2017). Future work is needed to determine what kinds of interventions are optimal to allow the brain to go back to using what is left in the lesioned hemisphere.

To date, TMS and tDCS studies aimed at enhancing motor recovery after stroke have had mixed results. It is possible that the models used as a basis for this research, focusing mainly on cortical regions, need to be updated to include the brainstem. With better neuroimaging techniques, a deeper understanding of the neural changes that occur in each individual brain is possible. With this knowledge, individualized models can be created and used to design personalized and multi-modal interventions that could include physical therapy, therapeutics, and stimulation. This approach may also be able to target specific types impairments, such as loss of independent joint control, which are hindering the patient the most.

In conclusion, the research presented in this dissertation demonstrates that after stroke there are degenerative changes in the lesioned hemisphere that expand well beyond the lesioned tissue as well as neuroplastic reorganizational structural and functional changes in the contralesional

brainstem and associated cortical regions. This neural rewiring correlates with a quantitative metric of independent joint control, suggesting that increased use of contralesional corticoreticulospinal pathways contributes to flexion synergy severity. It emphasizes the need to address the role that the brainstem plays after stroke and shows that the brainstem should be included into newer models of plastic reorganization of the motor system after brain injury. This better understanding of the neural mechanisms associated with loss of independent joint control in stroke informs clinical practice and can facilitate the development of more targeted and effective interventions for stroke rehabilitations.

References

Aja-Fernandez S, Alberola-Lopez C, Westin CF. Noise and signal estimation in magnitude MRI and Rician distributed images: a LMMSE approach. IEEE Trans Image Process 2008; 17: 1383-1398.

Alexander AL, Lee JE, Lazar M, Field AS. Diffusion tensor imaging of the brain. Neurotherapeutics 2007; 4: 316-329.

Ashburner J, Friston KJ. Voxel-based morphometry--the methods. Neuroimage 2000; 11: 805-821.

Baker SN. The primate reticulospinal tract, hand function and functional recovery. J Physiol 2011; 589: 5603-5612.

Baliki MN, Petre B, Torbey S, Herrmann KM, Huang L, Schnitzer TJ, *et al.* Corticostriatal functional connectivity predicts transition to chronic back pain. Nat Neurosci 2012; 15: 1117-1119.

Basser PJ, Mattiello J, LeBihan D. MR diffusion tensor spectroscopy and imaging. Biophys J 1994; 66: 259-267.

Battey TW, Karki M, Singhal AB, Wu O, Sadaghiani S, Campbell BC, *et al.* Brain edema predicts outcome after nonlacunar ischemic stroke. Stroke 2014; 45: 3643-3648.

Beer RF, Dewald JP, Dawson ML, Rymer WZ. Target-dependent differences between free and constrained arm movements in chronic hemiparesis. Exp Brain Res 2004; 156: 458-470.

Beer RF, Dewald JP, Rymer WZ. Deficits in the coordination of multijoint arm movements in patients with hemiparesis: evidence for disturbed control of limb dynamics. Exp Brain Res 2000; 131: 305-319.

Beer RF, Given JD, Dewald JP. Task-dependent weakness at the elbow in patients with hemiparesis. Arch Phys Med Rehabil 1999; 80: 766-772.

Behrens TE, Woolrich MW, Jenkinson M, Johansen-Berg H, Nunes RG, Clare S, *et al.* Characterization and propagation of uncertainty in diffusion-weighted MR imaging. Magn Reson Med 2003; 50: 1077-1088.

Belhaj-Saif A, Cheney PD. Plasticity in the distribution of the red nucleus output to forearm muscles after unilateral lesions of the pyramidal tract. J Neurophysiol 2000; 83: 3147-3153.

Bestmann S, Swayne O, Blankenburg F, Ruff CC, Teo J, Weiskopf N, *et al.* The role of contralesional dorsal premotor cortex after stroke as studied with concurrent TMS-fMRI. J Neurosci 2010; 30: 11926-11937.

Biswal B, Yetkin FZ, Haughton VM, Hyde JS. Functional connectivity in the motor cortex of resting human brain using echo-planar MRI. Magn Reson Med 1995; 34: 537-541.

Borich MR, Mang C, Boyd LA. Both projection and commissural pathways are disrupted in individuals with chronic stroke: investigating microstructural white matter correlates of motor recovery. BMC Neuroscience 2012; 13: 107.

Brunnstrom S. Movement therapy in hemiplegia: a neurophysiological approach. New York: Medical Dept.; 1970.

Butler AB, Hodos, W. Comparative Vertebrate Neuroanatomy: Evolution and Adaptation. 2005.

Calautti C, Baron JC. Functional neuroimaging studies of motor recovery after stroke in adults: a review. Stroke 2003; 34: 1553-1566.

Calautti C, Naccarato M, Jones PS, Sharma N, Day DD, Carpenter AT, *et al.* The relationship between motor deficit and hemisphere activation balance after stroke: A 3T fMRI study. Neuroimage 2007; 34: 322-331.

Canning CG, Ada L, Adams R, O'Dwyer NJ. Loss of strength contributes more to physical disability after stroke than loss of dexterity. Clin Rehabil 2004; 18: 300-308.

Carter AR, Astafiev SV, Lang CE, Connor LT, Rengachary J, Strube MJ, *et al.* Resting interhemispheric functional magnetic resonance imaging connectivity predicts performance after stroke. Ann Neurol 2010; 67: 365-375.

Chang EH, Argyelan M, Aggarwal M, Chandon TS, Karlsgodt KH, Mori S, *et al.* Diffusion tensor imaging measures of white matter compared to myelin basic protein immunofluorescence in tissue cleared intact brains. Data Brief 2017a; 10: 438-443.

Chang EH, Argyelan M, Aggarwal M, Chandon TS, Karlsgodt KH, Mori S, *et al.* The role of myelination in measures of white matter integrity: Combination of diffusion tensor imaging and two-photon microscopy of CLARITY intact brains. Neuroimage 2017b; 147: 253-261.

Chen AY, J., Dewald, J.P.A. A novel experimental setup combining EEG and robotics to investigate brain activity driving controlled reaching movements in chronic stroke survivors. IEEE 10th International Conference on Rehabilitation Robotics. 2007: 876-882.

Chen JL, Schlaug G. Resting state interhemispheric motor connectivity and white matter integrity correlate with motor impairment in chronic stroke. Front Neurol 2013; 4: 178.

Churchland MM, Yu BM, Ryu SI, Santhanam G, Shenoy KV. Neural variability in premotor cortex provides a signature of motor preparation. J Neurosci 2006; 26: 3697-3712.

Cisek P, Kalaska JF. Neural correlates of reaching decisions in dorsal premotor cortex: specification of multiple direction choices and final selection of action. Neuron 2005; 45: 801-814.

Concha L, Gross DW, Wheatley BM, Beaulieu C. Diffusion tensor imaging of time-dependent axonal and myelin degradation after corpus callosotomy in epilepsy patients. Neuroimage 2006; 32: 1090-1099.

Conn PM. Neuroscience in Medicine. Humana Press; 2008.

Cramer SC, Chopp M. Recovery recapitulates ontogeny. Trends Neurosci 2000; 23: 265-271.

Davidson AG, Buford JA. Bilateral actions of the reticulospinal tract on arm and shoulder muscles in the monkey: stimulus triggered averaging. Exp Brain Res 2006; 173: 25-39.

Davidson AG, Schieber MH, Buford JA. Bilateral spike-triggered average effects in arm and shoulder muscles from the monkey pontomedullary reticular formation. J Neurosci 2007; 27: 8053-8058.

Dayan E, Cohen LG. Neuroplasticity subserving motor skill learning. Neuron 2011; 72: 443-454.

Dewald JP, Beer RF. Abnormal joint torque patterns in the paretic upper limb of subjects with hemiparesis. Muscle Nerve 2001; 24: 273-283.

Dewald JP, Pope PS, Given JD, Buchanan TS, Rymer WZ. Abnormal muscle coactivation patterns during isometric torque generation at the elbow and shoulder in hemiparetic subjects. Brain 1995; 118 (Pt 2): 495-510.

Dewald JP, Sheshadri V, Dawson ML, Beer RF. Upper-limb discoordination in hemiparetic stroke: implications for neurorehabilitation. Top Stroke Rehabil 2001; 8: 1-12.

Draganski B, May A. Training-induced structural changes in the adult human brain. Behav Brain Res 2008; 192: 137-142.

Drew T, Dubuc R, Rossignol S. Discharge patterns of reticulospinal and other reticular neurons in chronic, unrestrained cats walking on a treadmill. J Neurophysiol 1986; 55: 375-401.

Dum RP, Strick PL. The origin of corticospinal projections from the premotor areas in the frontal lobe. J Neurosci 1991; 11: 667-689.

Dum RP, Strick PL. Motor areas in the frontal lobe of the primate. Physiol Behav 2002; 77: 677-682.

Dum RP, Strick PL. Frontal lobe inputs to the digit representations of the motor areas on the lateral surface of the hemisphere. J Neurosci 2005; 25: 1375-1386.

Ellis MD, Acosta AM, Yao J, Dewald JP. Position-dependent torque coupling and associated muscle activation in the hemiparetic upper extremity. Exp Brain Res 2007; 176: 594-602.

Ellis MD, Drogos J, Carmona C, Keller T, Dewald JP. Neck rotation modulates flexion synergy torques, indicating an ipsilateral reticulospinal source for impairment in stroke. J Neurophysiol 2012; 108: 3096-3104.

Ellis MD, Kottink AI, Prange GB, Rietman JS, Buurke JH, Dewald JP. Quantifying loss of independent joint control in acute stroke with a robotic evaluation of reaching workspace. Conf Proc IEEE Eng Med Biol Soc 2011; 2011: 8231-8234.

Ellis MD, Lan Y, Yao J, Dewald JP. Robotic quantification of upper extremity loss of independent joint control or flexion synergy in individuals with hemiparetic stroke: a review of paradigms addressing the effects of shoulder abduction loading. J Neuroeng Rehabil 2016; 13: 95.

Ellis MD, Sukal T, DeMott T, Dewald JP. Augmenting clinical evaluation of hemiparetic arm movement with a laboratory-based quantitative measurement of kinematics as a function of limb loading. Neurorehabil Neural Repair 2008; 22: 321-329.

Ellis MD, Sukal-Moulton T, Dewald JP. Progressive shoulder abduction loading is a crucial element of arm rehabilitation in chronic stroke. Neurorehabil Neural Repair 2009a; 23: 862-869.

Ellis MD, Sukal-Moulton TM, Dewald JP. Impairment-Based 3-D Robotic Intervention Improves Upper Extremity Work Area in Chronic Stroke: Targeting Abnormal Joint Torque Coupling With Progressive Shoulder Abduction Loading. IEEE Trans Robot 2009b; 25: 549-555.

Erdler M, Beisteiner R, Mayer D, Kaindl T, Edward V, Windischberger C, *et al.* Supplementary motor area activation preceding voluntary movement is detectable with a whole-scalp magnetoencephalography system. Neuroimage 2000; 11: 697-707.

Felten DL, Józefowicz RF. Netter's atlas of human neuroscience. Teterboro, N.J.: Icon Learning Systems; 2003.

Felton D, Jozefocicz, R. Netter's Atlas of Human Neuroscience. Elsevier Saunders; 2003.

Feys HM, De Weerdt WJ, Selz BE, Cox Steck GA, Spichiger R, Vereeck LE, *et al.* Effect of a therapeutic intervention for the hemiplegic upper limb in the acute phase after stroke: a single-blind, randomized, controlled multicenter trial. Stroke 1998; 29: 785-792.

Fox MD, Raichle ME. Spontaneous fluctuations in brain activity observed with functional magnetic resonance imaging. Nat Rev Neurosci 2007; 8: 700-711.

Fregosi M, Contestabile A, Hamadjida A, Rouiller EM. Corticobulbar projections from distinct motor cortical areas to the reticular formation in macaque monkeys. Eur J Neurosci 2017a.

Fregosi M, Contestabile A, Hamadjida A, Rouiller EM. Corticobulbar projections from distinct motor cortical areas to the reticular formation in macaque monkeys. Eur J Neurosci 2017b; 45: 1379-1395.

Fugl-Meyer AR, Jaasko L, Leyman I, Olsson S, Steglind S. The post-stroke hemiplegic patient. 1. a method for evaluation of physical performance. Scand J Rehabil Med 1975; 7: 13-31.

Given JD, Dewald JP, Rymer WZ. Joint dependent passive stiffness in paretic and contralateral limbs of spastic patients with hemiparetic stroke. J Neurol Neurosurg Psychiatry 1995; 59: 271-279.

Gladstone DJ, Danells CJ, Black SE. The fugl-meyer assessment of motor recovery after stroke: a critical review of its measurement properties. Neurorehabil Neural Repair 2002; 16: 232-240.

Globas C, Lam JM, Zhang W, Imanbayev A, Hertler B, Becker C, et al. Mesencephalic corticospinal atrophy predicts baseline deficit but not response to unilateral or bilateral arm training in chronic stroke. Neurorehabil Neural Repair 2011; 25: 81-87.

Go AS, Mozaffarian D, Roger VL, Benjamin EJ, Berry JD, Blaha MJ, et al. Heart disease and stroke statistics--2014 update: a report from the American Heart Association. Circulation 2014; 129: e28-e292.

Grefkes C, Nowak DA, Eickhoff SB, Dafotakis M, Kust J, Karbe H, et al. Cortical connectivity after subcortical stroke assessed with functional magnetic resonance imaging. Ann Neurol 2008; 63: 236-246.

Greve DN, Fischl B. Accurate and robust brain image alignment using boundary-based registration. Neuroimage 2009; 48: 63-72.

Groisser BN, Copen WA, Singhal AB, Hirai KK, Schaechter JD. Corticospinal tract diffusion abnormalities early after stroke predict motor outcome. Neurorehabil Neural Repair 2014; 28: 751-760.

Hoover JE, Strick PL. Multiple output channels in the basal ganglia. Science 1993; 259: 819-821.

Hua K, Zhang J, Wakana S, Jiang H, Li X, Reich DS, et al. Tract probability maps in stereotaxic spaces: analyses of white matter anatomy and tract-specific quantification. Neuroimage 2008; 39: 336-347.

Humphrey DR, Gold R, Reed DJ. Sizes, laminar and topographic origins of cortical projections to the major divisions of the red nucleus in the monkey. J Comp Neurol 1984; 225: 75-94.

Ingo C, Magin RL, Colon-Perez L, Triplett W, Mareci TH. On random walks and entropy in diffusion-weighted magnetic resonance imaging studies of neural tissue. Magn Reson Med 2014; 71: 617-627.

Jang SH, Seo JP. The distribution of the cortical origin of the corticoreticular pathway in the human brain: a diffusion tensor imaging study. Somatosens Mot Res 2014; 31: 204-208.

Jang SH, Seo JP. The anatomical location of the corticoreticular pathway at the subcortical white matter in the human brain: A diffusion tensor imaging study. Somatosens Mot Res 2015; 32: 106-109.

Jason E, Dastidar P, Kalliokoski A, Luukkaala T, Soimakallio S. Diffusion tensor imaging of chronic right cerebral hemisphere infarctions. J Neuroimaging 2011; 21: 325-331.

Jenkinson M, Bannister P, Brady M, Smith S. Improved optimization for the robust and accurate linear registration and motion correction of brain images. Neuroimage 2002; 17: 825-841.

Jenkinson M, Smith S. A global optimisation method for robust affine registration of brain images. Med Image Anal 2001; 5: 143-156.

Johansen-Berg H, Behrens TEJ. Diffusion MRI : from quantitative measurement to in-vivo neuroanatomy. London, UK ; Waltham, MA: Elsevier/Academic Press; 2014.

Johansen-Berg H, Rushworth MF, Bogdanovic MD, Kischka U, Wimalaratna S, Matthews PM. The role of ipsilateral premotor cortex in hand movement after stroke. Proc Natl Acad Sci U S A 2002; 99: 14518-14523.

Jones DK, Knosche TR, Turner R. White matter integrity, fiber count, and other fallacies: the do's and don'ts of diffusion MRI. Neuroimage 2013; 73: 239-254.

Kandel ER. Principles of neural science. New York: McGraw-Hill; 2013.

Keizer K, Kuypers HG. Distribution of corticospinal neurons with collaterals to lower brain stem reticular formation in cat. Exp Brain Res 1984; 54: 107-120.

Keizer K, Kuypers HG. Distribution of corticospinal neurons with collaterals to the lower brain stem reticular formation in monkey (Macaca fascicularis). Exp Brain Res 1989; 74: 311-318.

Kennedy PR, Gibson AR, Houk JC. Functional and anatomic differentiation between parvicellular and magnocellular regions of red nucleus in the monkey. Brain Res 1986; 364: 124-136.

Krainak DM, Ellis MD, Bury K, Churchill S, Pavlovics E, Pearson L, et al. Effects of body orientation on maximum voluntary arm torques. Muscle Nerve 2011; 44: 805-813.

Kuhtz-Buschbeck JP, Mahnkopf C, Holzknecht C, Siebner H, Ulmer S, Jansen O. Effector-independent representations of simple and complex imagined finger movements: a combined fMRI and TMS study. Eur J Neurosci 2003; 18: 3375-3387.

Lan YY, J; Dewald, J.P. The Impact of Shoulder Abduction Loading on Volitional Hand Opening and Grasping in Chronic Hemiparetic Stroke. Neurorehabilitation & Neural Repair 2017; In Press.

Lawrence DG, Kuypers HG. The functional organization of the motor system in the monkey. I. The effects of bilateral pyramidal lesions. Brain 1968a; 91: 1-14.

Lawrence DG, Kuypers HG. The functional organization of the motor system in the monkey. II. The effects of lesions of the descending brain-stem pathways. Brain 1968b; 91: 15-36.

Lefebvre S, Dricot L, Laloux P, Desfontaines P, Evrard F, Peeters A, et al. Increased functional connectivity one week after motor learning and tDCS in stroke patients. Neuroscience 2017; 340: 424-435.

Lemon RN. Descending pathways in motor control. Annu Rev Neurosci 2008; 31: 195-218.

Leopold DA, Maier A. Ongoing physiological processes in the cerebral cortex. Neuroimage 2012; 62: 2190-2200.

Li Y, Wu P, Liang F, Huang W. The microstructural status of the corpus callosum is associated with the degree of motor function and neurological deficit in stroke patients. PLoS One 2015; 10: e0122615.

Lindenberg R, Zhu LL, Ruber T, Schlaug G. Predicting functional motor potential in chronic stroke patients using diffusion tensor imaging. Hum Brain Mapp 2012; 33: 1040-1051.

Logothetis NK, Pfeuffer J. On the nature of the BOLD fMRI contrast mechanism. Magn Reson Imaging 2004; 22: 1517-1531.

Lotze M, Kaethner RJ, Erb M, Cohen LG, Grodd W, Topka H. Comparison of representational maps using functional magnetic resonance imaging and transcranial magnetic stimulation. Clin Neurophysiol 2003; 114: 306-312.

Margulies DS, Kelly AM, Uddin LQ, Biswal BB, Castellanos FX, Milham MP. Mapping the functional connectivity of anterior cingulate cortex. Neuroimage 2007; 37: 579-588.

Matsuyama K, Drew T. Vestibulospinal and reticulospinal neuronal activity during locomotion in the intact cat. I. Walking on a level surface. J Neurophysiol 2000; 84: 2237-2256.

Mayka MA, Corcos DM, Leurgans SE, Vaillancourt DE. Three-dimensional locations and boundaries of motor and premotor cortices as defined by functional brain imaging: a meta-analysis. Neuroimage 2006; 31: 1453-1474.

McMorland AJ, Runnalls KD, Byblow WD. A neuroanatomical framework for upper limb synergies after stroke. Front Hum Neurosci 2015; 9: 82.

McPherson JG, Ellis MD, Heckman CJ, Dewald JP. Evidence for increased activation of persistent inward currents in individuals with chronic hemiparetic stroke. J Neurophysiol 2008; 100: 3236-3243.

Meola A, Yeh FC, Fellows-Mayle W, Weed J, Fernandez-Miranda JC. Human Connectome-Based Tractographic Atlas of the Brainstem Connections and Surgical Approaches. Neurosurgery 2016; 79: 437-455.

Middleton FA, Strick PL. Cerebellar output: motor and cognitive channels. Trends Cogn Sci 1998; 2: 348-354.

Miller LC, Dewald JP. Involuntary paretic wrist/finger flexion forces and EMG increase with shoulder abduction load in individuals with chronic stroke. Clin Neurophysiol 2012; 123: 1216-1225.

Montgomery LR. (2013). *Role of the Reticulospinal and Corticoreticular Systems for the Control of Reaching in Non Human Primates.* (Degree of Doctor of Philosophy), Ohio State University.

Montgomery LR, Herbert WJ, Buford JA. Recruitment of ipsilateral and contralateral upper limb muscles following stimulation of the cortical motor areas in the monkey. Exp Brain Res 2013; 230: 153-164.

Mori S. MRI atlas of human white matter. Amsterdam ; Boston: Elsevier; 2005.

Mori S, Matsuyama K, Mori F, Nakajima K. Supraspinal sites that induce locomotion in the vertebrate central nervous system. Adv Neurol 2001; 87: 25-40.

Mori S, Zhang J. Principles of diffusion tensor imaging and its applications to basic neuroscience research. Neuron 2006; 51: 527-539.

Mozaffarian D, Benjamin EJ, Go AS, Arnett DK, Blaha MJ, Cushman M, *et al.* Heart Disease and Stroke Statistics-2016 Update: A Report From the American Heart Association. Circulation 2016; 133: e38-360.

Murata A, Fadiga L, Fogassi L, Gallese V, Raos V, Rizzolatti G. Object representation in the ventral premotor cortex (area F5) of the monkey. J Neurophysiol 1997; 78: 2226-2230.

Mutso AA, Petre B, Huang L, Baliki MN, Torbey S, Herrmann KM, *et al.* Reorganization of hippocampal functional connectivity with transition to chronic back pain. J Neurophysiol 2014; 111: 1065-1076.

Nathan PW, Smith MC. Long descending tracts in man. I. Review of present knowledge. Brain 1955; 78: 248-303.

Nathan PW, Smith MC. The rubrospinal and central tegmental tracts in man. Brain 1982; 105: 223-269.

Nijboer TCW, Buma FE, Winters C, Vansteensel MJ, Kwakkel G, Ramsey NF, *et al.* No changes in functional connectivity during motor recovery beyond 5 weeks after stroke; A longitudinal resting-state fMRI study. PLoS One 2017; 12: e0178017.

Ogawa S, Lee TM, Kay AR, Tank DW. Brain magnetic resonance imaging with contrast dependent on blood oxygenation. Proc Natl Acad Sci U S A 1990; 87: 9868-9872.

Ogawa S, Menon RS, Tank DW, Kim SG, Merkle H, Ellermann JM, *et al.* Functional brain mapping by blood oxygenation level-dependent contrast magnetic resonance imaging. A comparison of signal characteristics with a biophysical model. Biophys J 1993; 64: 803-812.

Onodera S, Hicks TP. Carbocyanine dye usage in demarcating boundaries of the aged human red nucleus. PLoS One 2010; 5: e14430.

Opheim A, Danielsson A, Alt Murphy M, Persson HC, Sunnerhagen KS. Upper-limb spasticity during the first year after stroke: stroke arm longitudinal study at the University of Gothenburg. Am J Phys Med Rehabil 2014; 93: 884-896.

Owen M, Ingo C, Dewald JPA. Upper Extremity Motor Impairments and Microstructural Changes in Bulbospinal Pathways in Chronic Hemiparetic Stroke. Front Neurol 2017; 8: 257.

Park CH, Chang WH, Ohn SH, Kim ST, Bang OY, Pascual-Leone A, *et al.* Longitudinal changes of resting-state functional connectivity during motor recovery after stroke. Stroke 2011; 42: 1357-1362.

Pascual-Leone A, Amedi A, Fregni F, Merabet LB. The plastic human brain cortex. Annu Rev Neurosci 2005; 28: 377-401.

Prentice SD, Drew T. Contributions of the reticulospinal system to the postural adjustments occurring during voluntary gait modifications. J Neurophysiol 2001; 85: 679-698.

Puig J, Blasco G, Daunis IEJ, Thomalla G, Castellanos M, Figueras J, *et al.* Decreased corticospinal tract fractional anisotropy predicts long-term motor outcome after stroke. Stroke 2013; 44: 2016-2018.

Qiu M, Darling WG, Morecraft RJ, Ni CC, Rajendra J, Butler AJ. White matter integrity is a stronger predictor of motor function than BOLD response in patients with stroke. Neurorehabil Neural Repair 2011; 25: 275-284.

Raichle ME. Cognitive neuroscience. Bold insights. Nature 2001; 412: 128-130.

Raichle ME, MacLeod AM, Snyder AZ, Powers WJ, Gusnard DA, Shulman GL. A default mode of brain function. Proc Natl Acad Sci U S A 2001; 98: 676-682.

Rehme AK, Eickhoff SB, Rottschy C, Fink GR, Grefkes C. Activation likelihood estimation meta-analysis of motor-related neural activity after stroke. Neuroimage 2012; 59: 2771-2782.

Riddle CN, Baker SN. Convergence of pyramidal and medial brain stem descending pathways onto macaque cervical spinal interneurons. J Neurophysiol 2010; 103: 2821-2832.

Riddle CN, Edgley SA, Baker SN. Direct and indirect connections with upper limb motoneurons from the primate reticulospinal tract. J Neurosci 2009; 29: 4993-4999.

Ruber T, Schlaug G, Lindenberg R. Compensatory role of the cortico-rubro-spinal tract in motor recovery after stroke. Neurology 2012; 79: 515-522.

Schaechter JD, Fricker ZP, Perdue KL, Helmer KG, Vangel MG, Greve DN, *et al.* Microstructural status of ipsilesional and contralesional corticospinal tract correlates with motor skill in chronic stroke patients. Hum Brain Mapp 2009; 30: 3461-3474.

Schepens B, Drew T. Independent and convergent signals from the pontomedullary reticular formation contribute to the control of posture and movement during reaching in the cat. J Neurophysiol 2004; 92: 2217-2238.

Schepens B, Stapley P, Drew T. Neurons in the pontomedullary reticular formation signal posture and movement both as an integrated behavior and independently. J Neurophysiol 2008; 100: 2235-2253.

Scholz J, Klein MC, Behrens TE, Johansen-Berg H. Training induces changes in white-matter architecture. Nat Neurosci 2009; 12: 1370-1371.

Schulz R, Park E, Lee J, Chang WH, Lee A, Kim YH, *et al.* Synergistic but independent: The role of corticospinal and alternate motor fibers for residual motor output after stroke. Neuroimage Clin 2017; 15: 118-124.

Schwerin S, Dewald JP, Haztl M, Jovanovich S, Nickeas M, MacKinnon C. Ipsilateral versus contralateral cortical motor projections to a shoulder adductor in chronic hemiparetic stroke: implications for the expression of arm synergies. Exp Brain Res 2008; 185: 509-519.

Schwerin SC, Yao J, Dewald JP. Using paired pulse TMS to facilitate contralateral and ipsilateral MEPs in upper extremity muscles of chronic hemiparetic stroke patients. J Neurosci Methods 2011; 195: 151-160.

Seo JP, Jang SH. Different characteristics of the corticospinal tract according to the cerebral origin: DTI study. AJNR Am J Neuroradiol 2013; 34: 1359-1363.

Shaw CM, Alvord EC, Jr., Berry RG. Swelling of the brain following ischemic infarction with arterial occlusion. Arch Neurol 1959; 1: 161-177.

Smith SM, Jenkinson M, Johansen-Berg H, Rueckert D, Nichols TE, Mackay CE, *et al.* Tract-based spatial statistics: voxelwise analysis of multi-subject diffusion data. Neuroimage 2006; 31: 1487-1505.

Smith SM, Jenkinson M, Woolrich MW, Beckmann CF, Behrens TE, Johansen-Berg H, *et al.* Advances in functional and structural MR image analysis and implementation as FSL. Neuroimage 2004; 23 Suppl 1: S208-219.

Song F, Zhang F, Yin DZ, Hu YS, Fan MX, Ni HH, *et al.* Diffusion tensor imaging for predicting hand motor outcome in chronic stroke patients. J Int Med Res 2012; 40: 126-133.

Song SK, Sun SW, Ju WK, Lin SJ, Cross AH, Neufeld AH. Diffusion tensor imaging detects and differentiates axon and myelin degeneration in mouse optic nerve after retinal ischemia. Neuroimage 2003; 20: 1714-1722.

Robust web-based parallel-optimized minimal pre-processing and analyzing pipeline for fMRI big data. OHBM 2015.

Standring S. Gray's anatomy : the anatomical basis of clinical practice. 2016.

Stinear CM, Barber PA, Smale PR, Coxon JP, Fleming MK, Byblow WD. Functional potential in chronic stroke patients depends on corticospinal tract integrity. Brain 2007; 130: 170-180.

Sukal TM, Ellis MD, Dewald JP. Shoulder abduction-induced reductions in reaching work area following hemiparetic stroke: neuroscientific implications. Exp Brain Res 2007; 183: 215-223.

Takenobu Y, Hayashi T, Moriwaki H, Nagatsuka K, Naritomi H, Fukuyama H. Motor recovery and microstructural change in rubro-spinal tract in subcortical stroke. Neuroimage Clin 2014; 4: 201-208.

Taubert M, Draganski B, Anwander A, Muller K, Horstmann A, Villringer A, *et al.* Dynamic properties of human brain structure: learning-related changes in cortical areas and associated fiber connections. J Neurosci 2010; 30: 11670-11677.

Thiel A, Vahdat S. Structural and resting-state brain connectivity of motor networks after stroke. Stroke 2015; 46: 296-301.

Twitchell TE. The restoration of motor function following hemiplegia in man. Brain 1951; 74: 443-480.

Urbin MA, Hong X, Lang CE, Carter AR. Resting-state functional connectivity and its association with multiple domains of upper-extremity function in chronic stroke. Neurorehabil Neural Repair 2014; 28: 761-769.

Vahdat S, Darainy M, Milner TE, Ostry DJ. Functionally specific changes in resting-state sensorimotor networks after motor learning. J Neurosci 2011; 31: 16907-16915.

Velozo CA, Woodbury ML. Translating measurement findings into rehabilitation practice: an example using Fugl-Meyer Assessment-Upper Extremity with patients following stroke. J Rehabil Res Dev 2011; 48: 1211-1222.

Wakana S, Caprihan A, Panzenboeck MM, Fallon JH, Perry M, Gollub RL, *et al.* Reproducibility of quantitative tractography methods applied to cerebral white matter. Neuroimage 2007; 36: 630-644.

Wan CY, Zheng X, Marchina S, Norton A, Schlaug G. Intensive therapy induces contralateral white matter changes in chronic stroke patients with Broca's aphasia. Brain Lang 2014; 136: 1-7.

Wang B, Wang X, Katsaggelos AK, Parrish T. (2015). *Automatic Segmentation of Chronic Stroke Employing 3D Mean-Shift and Symmetry of the Human Brain.* Paper presented at the Hum Brain Mapp.

Ward NS, Brown MM, Thompson AJ, Frackowiak RS. Neural correlates of motor recovery after stroke: a longitudinal fMRI study. Brain 2003a; 126: 2476-2496.

Ward NS, Brown MM, Thompson AJ, Frackowiak RS. Neural correlates of outcome after stroke: a cross-sectional fMRI study. Brain 2003b; 126: 1430-1448.

Ward NS, Cohen LG. Mechanisms underlying recovery of motor function after stroke. Arch Neurol 2004; 61: 1844-1848.

Webb AR. Introduction to biomedical imaging. Hoboken, New Jersey: Wiley; 2003.

Welniarz Q, Dusart I, Roze E. The corticospinal tract: Evolution, development, and human disorders. Dev Neurobiol 2017; 77: 810-829.

Wen H, Alshikho MJ, Wang Y, Luo X, Zafonte R, Herbert MR, *et al.* Correlation of Fractional Anisotropy With Motor Recovery in Patients With Stroke After Postacute Rehabilitation. Arch Phys Med Rehabil 2016; 97: 1487-1495.

Whitwell JL. Voxel-based morphometry: an automated technique for assessing structural changes in the brain. J Neurosci 2009; 29: 9661-9664.

Wilkins KO, M., Ingo, C., Carmona, C., Dewald, J., Yao, J. Neural Plasticity in Moderate to Severe Chronic Stroke Following a Device-Assisted Task-Specific Arm/Hand Intervention. Front Neurol 2017.

Winkler AM, Ridgway GR, Webster MA, Smith SM, Nichols TE. Permutation inference for the general linear model. Neuroimage 2014; 92: 381-397.

Wittenberg GF, Richards LG, Jones-Lush LM, Roys SR, Gullapalli RP, Yang S, *et al.* Predictors and brain connectivity changes associated with arm motor function improvement from intensive practice in chronic stroke. F1000Res 2016; 5: 2119.

Zaaimi B, Edgley SA, Soteropoulos DS, Baker SN. Changes in descending motor pathway connectivity after corticospinal tract lesion in macaque monkey. Brain 2012; 135: 2277-2289.

Appendix

Northwestern University Feinberg School of Medicine

**Physical Therapy and
Human Movement Sciences**

Protocol.   PI.   Participant.

ARM MOTOR FUGL-MEYER

Session

Assessment Date: _____ _____ / _____ _____ / _____ _____   Assessment Time: _____ _____ _____ _____
　　　　　　　　　　 MM　　　　DD　　　　YY　　　　　　　　　　　　　　　　　　　(Military Time)

The Arm Motor Fugal- Myer Motor Assessment Manual will be used

	0		2
I. Reflex Activity (0 = no reflex activity elicited, 2 = reflex activity can be elicited)			
Biceps Flexor			
Triceps Extensor			
II. Dynamic Movement Within Flexor Synergy	0	1	2
Retraction			
Elevation			
Abduction			
External Rotation			
Elbow Flexion			
Supination			
III. Dynamic Movement Within Extensor Synergy	0	1	2
Adduction/Internal Rotation			
Elbow Extension			
Pronation			
IV. Movement Mixing Flexion and Extension Synergies	0	1	2
Hand to lumbar spine			
Shoulder flexion to 90_0 with elbow at 0_0 and forearm in neutral			
Pronation/Supination with elbow at 90_0			

Physical Therapy and
Human Movement Sciences

Northwestern University Feinberg School of Medicine

Protocol._____ PI._____ Participant.

	0	1	2
V. Movement With Little Or No Synergy Dependence			
Abduction to 90.			
Shoulder flexion 90. to 180. with elbow at 0. and forearm in neutral			
Pronation/Supination with elbow at 0. and shoulder between 30. and 90. of flexion			
VI. Normal Reflex Activity	0	1	2
Test deep tendon reflexes of the biceps, long finger flexors, and triceps			
VII. Wrist Stability and Mobility	0	1	2
Wrist stability with wrist in 15. extension and elbow at 90.			
Wrist mobility with the elbow at 90.			
Wrist stability with wrist in 15. extension and elbow at 0. and shoulder between 30. and 90. of flexion			
Wrist mobility with the elbow at 0. and the shoulder between 30. and 90. of			
flexion Circumduction of the wrist			
VIII. Hand	0	1	2
Mass flexion			
Mass extension			
Grasp A (hook)			
Grasp B (thumb adduction)			
Grasp C (1st and 2nd digit pulpa approximation)			
Grasp D (1st and 2nd digit cylindrical)			
Grasp E (spherical)			

Northwestern University Feinberg School of Medicine

**Physical Therapy and
Human Movement Sciences**

Protocol. _____ PI. _____ Participant. _____

IX. Coordination/Speed	0	1	2
Tremor			
Dysmetria			
Definition of Speed Time Speed: Left _____ sec. Right _____ sec 0 = a time difference of 6.00 and greater 1 = a time difference between 2.00 and 5.99 seconds 2 = a time difference of less than 2.00 seconds			

ARM MOTOR TOTAL SCORE	_____ /66 points

COMMENTS:

_____
_____
_____
_____
_____
_____

CLINICIAN SIGNATURE AND PRINTED NAME   DATE